

Recent Advances on Viability and Antifragility in Project Scheduling

Lead Guest Editor: Reza Lotfi

Guest Editors: Gerhard-Wilhelm Weber and Eren Özceylan





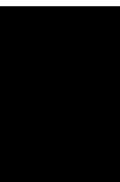
Recent Advances on Viability and Antifragility in Project Scheduling

Advances in Civil Engineering

Recent Advances on Viability and Antifragility in Project Scheduling

Lead Guest Editor: Reza Lotfi

Guest Editors: Gerhard-Wilhelm Weber and Eren Özceylan



Copyright © 2023 Hindawi Limited. All rights reserved.

This is a special issue published in "Advances in Civil Engineering." All articles are open access articles distributed under the Creative Commons Attribution License, which permits unrestricted use, distribution, and reproduction in any medium, provided the original work is properly cited.






Chief Editor

Cumaraswamy Vipulanandan, USA










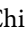



Associate Editors

Chiara Bedon , Italy
Constantin Chalioris , Greece
Ghassan Chehab , Lebanon
Ottavia Corbi, Italy
Mohamed ElGawady , USA
Husnain Haider , Saudi Arabia
Jian Ji , China
Jiang Jin , China
Shazim A. Memon , Kazakhstan
Hossein Moayedi , Vietnam
Sanjay Nimbalkar, Australia
Giuseppe Oliveto , Italy
Alessandro Palmeri , United Kingdom
Arnaud Perrot , France
Hugo Rodrigues , Portugal
Victor Yepes , Spain
Xianbo Zhao , Australia

Academic Editors

José A.F.O. Correia, Portugal
Glenda Abate, Italy
Khalid Abdel-Rahman , Germany
Ali Mardani Aghabaglou, Turkey
José Aguiar , Portugal
Afaq Ahmad , Pakistan
Muhammad Riaz Ahmad , Hong Kong
Hashim M.N. Al-Madani , Bahrain
Luigi Aldieri , Italy
Angelo Aloisio , Italy
Maria Cruz Alonso, Spain
Filipe Amarante dos Santos , Portugal
Serji N. Amirkhania, USA
Eleftherios K. Anastasiou , Greece
Panagiotis Ch. Anastasopoulos , USA
Mohamed Moafak Arbili , Iraq
Farhad Aslani , Australia
Siva Avudaiappan , Chile
Ozgur BASKAN , Turkey
Adewumi Babafemi, Nigeria
Morteza Bagherpour, Turkey
Qingsheng Bai , Germany
Nicola Baldo , Italy
Daniele Baraldi , Italy

Eva Barreira , Portugal
Emilio Bastidas-Arteaga , France
Rita Bento, Portugal
Rafael Bergillos , Spain
Han-bing Bian , China
Xia Bian , China
Huseyin Bilgin , Albania
Giovanni Biondi , Italy
Hugo C. Biscaia , Portugal
Rahul Biswas , India
Edén Bojórquez , Mexico
Giosuè Boscato , Italy
Melina Bosco , Italy
Jorge Branco , Portugal
Bruno Briseghella , China
Brian M. Broderick, Ireland
Emanuele Brunesi , Italy
Quoc-Bao Bui , Vietnam
Tan-Trung Bui , France
Nicola Buratti, Italy
Gaochuang Cai, France
Gladis Camarini , Brazil
Alberto Campisano , Italy
Qi Cao, China
Qixin Cao, China
Iacopo Carnacina , Italy
Alessio Cascardi, Italy
Paolo Castaldo , Italy
Nicola Cavalagli , Italy
Liborio Cavaleri , Italy
Anush Chandrappa , United Kingdom
Wen-Shao Chang , United Kingdom
Muhammad Tariq Amin Chaudhary, Kuwait
Po-Han Chen , Taiwan
Qian Chen , China
Wei Tong Chen , Taiwan
Qixiu Cheng, Hong Kong
Zhanbo Cheng, United Kingdom
Nicholas Chileshe, Australia
Prinya Chindaprasirt , Thailand
Corrado Chisari , United Kingdom
Se Jin Choi , Republic of Korea
Heap-Yih Chong , Australia
S.H. Chu , USA
Ting-Xiang Chu , China

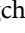
Zhaofei Chu , China
Wonseok Chung , Republic of Korea
Donato Ciampa , Italy
Gian Paolo Cimellaro, Italy
Francesco Colangelo, Italy
Romulus Costache , Romania
Liviu-Adrian Cotfas , Romania
Antonio Maria D'Altri, Italy
Bruno Dal Lago , Italy
Amos Darko , Hong Kong
Arka Jyoti Das , India
Dario De Domenico , Italy
Gianmarco De Felice , Italy
Stefano De Miranda , Italy
Maria T. De Risi , Italy
Tayfun Dede, Turkey
Sadik O. Degertekin , Turkey
Camelia Delcea , Romania
Cristoforo Demartino, China
Giuseppe Di Filippo , Italy
Luigi Di Sarno, Italy
Fabio Di Trapani , Italy
Aboelkasim Diab , Egypt
Thi My Dung Do, Vietnam
Giulio Dondi , Italy
Jiangfeng Dong , China
Chao Dou , China
Mario D'Aniello , Italy
Jingtao Du , China
Ahmed Elghazouli, United Kingdom
Francesco Fabbrocino , Italy
Flora Faleschini , Italy
Dingqiang Fan, Hong Kong
Xueping Fan, China
Qian Fang , China
Salar Farahmand-Tabar , Iran
Ilenia Farina, Italy
Roberto Fedele, Italy
Guang-Liang Feng , China
Luigi Fenu , Italy
Tiago Ferreira , Portugal
Marco Filippo Ferrotto, Italy
Antonio Formisano , Italy
Guoyang Fu, Australia
Stefano Galassi , Italy

Junfeng Gao , China
Meng Gao , China
Giovanni Garcea , Italy
Enrique García-Macías, Spain
Emilio García-Taengua , United Kingdom
DongDong Ge , USA
Khaled Ghaedi, Malaysia
Khaled Ghaedi , Malaysia
Gian Felice Giaccu, Italy
Agathoklis Giaralis , United Kingdom
Ravindran Gobinath, India
Rodrigo Gonçalves, Portugal
Peilin Gong , China
Belén González-Fonteboa , Spain
Salvatore Grasso , Italy
Fan Gu, USA
Erhan Güneyisi , Turkey
Esra Mete Güneyisi, Turkey
Pingye Guo , China
Ankit Gupta , India
Federico Gusella , Italy
Kemal Hacıfendioglu, Turkey
Jianyong Han , China
Song Han , China
Asad Hanif , Macau
Hadi Hasanzadehshooiili , Canada
Mostafa Fahmi Hassanein, Egypt
Amir Ahmad Hedayat , Iran
Khandaker Hossain , Canada
Zahid Hossain , USA
Chao Hou, China
Biao Hu, China
Jiang Hu , China
Xiaodong Hu, China
Lei Huang , China
Cun Hui , China
Bon-Gang Hwang, Singapore
Jijo James , India
Abbas Fadhil Jasim , Iraq
Ahad Javanmardi , China
Krishnan Prabhakan Jaya, India
Dong-Sheng Jeng , Australia
Han-Yong Jeon, Republic of Korea
Pengjiao Jia, China
Shaohua Jiang , China

MOUSTAFA KASSEM , Malaysia
Mosbeh Kaloop , Egypt
Shankar Karuppanan , Ethiopia
John Kechagias , Greece
Mohammad Khajehzadeh , Iran
Afzal Husain Khan , Saudi Arabia
Mehran Khan , Hong Kong
Manoj Khandelwal, Australia
Jin Kook Kim , Republic of Korea
Woosuk Kim , Republic of Korea
Vaclav Koci , Czech Republic
Loke Kok Foong, Vietnam
Hailing Kong , China
Leonidas Alexandros Kouris , Greece
Kyriakos Kourousis , Ireland
Moacir Kripka , Brazil
Anupam Kumar, The Netherlands
Emma La Malfa Ribolla, Czech Republic
Ali Lakirouhani , Iran
Angus C. C. Lam, China
Thanh Quang Khai Lam , Vietnam
Luciano Lamberti, Italy
Andreas Lampropoulos , United Kingdom
Raffaele Landolfo, Italy
Massimo Latour , Italy
Bang Yeon Lee , Republic of Korea
Eul-Bum Lee , Republic of Korea
Zhen Lei , Canada
Leonardo Leonetti , Italy
Chun-Qing Li , Australia
Dongsheng Li , China
Gen Li, China
Jiale Li , China
Minghui Li, China
Qingchao Li , China
Shuang Yang Li , China
Sunwei Li , Hong Kong
Yajun Li , China
Shun Liang , China
Francesco Liguori , Italy
Jae-Han Lim , Republic of Korea
Jia-Rui Lin , China
Kun Lin , China
Shibin Lin, China

Tzu-Kang Lin , Taiwan
Yu-Cheng Lin , Taiwan
Hexu Liu, USA
Jian Lin Liu , China
Xiaoli Liu , China
Xuemei Liu , Australia
Zaobao Liu , China
Zhuang-Zhuang Liu, China
Diego Lopez-Garcia , Chile
Cristiano Loss , Canada
Lyan-Ywan Lu , Taiwan
Jin Luo , USA
Yanbin Luo , China
Jianjun Ma , China
Junwei Ma , China
Tian-Shou Ma, China
Zhongguo John Ma , USA
Maria Macchiaroli, Italy
Domenico Magisano, Italy
Reza Mahinroosta, Australia
Yann Malecot , France
Prabhat Kumar Mandal , India
John Mander, USA
Iman Mansouri, Iran
André Dias Martins, Portugal
Domagoj Matesan , Croatia
Jose Matos, Portugal
Vasant Matsagar , India
Claudio Mazzotti , Italy
Ahmed Mebarki , France
Gang Mei , China
Kasim Mermerdas, Turkey
Giovanni Minafò , Italy
Masoomah Mirrashid , Iran
Abbas Mohajerani , Australia
Fadzli Mohamed Nazri , Malaysia
Fabrizio Mollaioli , Italy
Rosario Montuori , Italy
H. Naderpour , Iran
Hassan Nasir , Pakistan
Hossein Nassiraei , Iran
Satheeskumar Navaratnam , Australia
Ignacio J. Navarro , Spain
Ashish Kumar Nayak , India
Behzad Nematollahi , Australia

Chayut Ngamkhanong , Thailand
Trung Ngo, Australia
Tengfei Nian, China
Mehdi Nikoo , Canada
Youjun Ning , China
Olugbenga Timo Oladinrin , United Kingdom
Oladimeji Benedict Olalusi, South Africa
Timothy O. Olawumi , Hong Kong
Alejandro Orfila , Spain
Maurizio Orlando , Italy
Siti Aminah Osman, Malaysia
Walid Oueslati , Tunisia
SUVASH PAUL , Bangladesh
John-Paris Pantouvakis , Greece
Fabrizio Paolacci , Italy
Giuseppina Pappalardo , Italy
Fulvio Parisi , Italy
Dimitrios G. Pavlou , Norway
Daniele Pellegrini , Italy
Gatheeshgar Perampalam , United Kingdom
Daniele Perrone , Italy
Giuseppe Piccardo , Italy
Vagelis Plevris , Qatar
Andrea Pranno , Italy
Adolfo Preciado , Mexico
Chongchong Qi , China
Yu Qian, USA
Ying Qin , China
Giuseppe Quaranta , Italy
Krishanu ROY , New Zealand
Vlastimir Radonjanin, Serbia
Carlo Rainieri , Italy
Rahul V. Ralegaonkar, India
Raizal Saifulnaz Muhammad Rashid, Malaysia
Alessandro Rasulo , Italy
Chonghong Ren , China
Qing-Xin Ren, China
Dimitris Rizos , USA
Geoffrey W. Rodgers , New Zealand
Pier Paolo Rossi, Italy
Nicola Ruggieri , Italy
JUNLONG SHANG, Singapore



Nikhil Saboo, India
Anna Saetta, Italy
Juan Sagaseta , United Kingdom
Timo Saksala, Finland
Mostafa Salari, Canada
Ginevra Salerno , Italy
Evangelos J. Sapountzakis , Greece
Vassilis Sarhosis , United Kingdom
Navaratnarajah Sathiparan , Sri Lanka
Fabrizio Scozzese , Italy
Halil Sezen , USA
Payam Shafigh , Malaysia
M. Shahria Alam, Canada
Yi Shan, China
Hussein Sharaf, Iraq
Mostafa Sharifzadeh, Australia
Sanjay Kumar Shukla, Australia
Amir Si Larbi , France
Okan Sirin , Qatar
Piotr Smarzewski , Poland
Francesca Sollecito , Italy
Rui Song , China
Tian-Yi Song, Australia
Flavio Stochino , Italy
Mayank Sukhija , USA
Piti Sukontasukkul , Thailand
Jianping Sun, Singapore
Xiao Sun , China
T. Tafsirojjaman , Australia
Fujiao Tang , China
Patrick W.C. Tang , Australia
Zhi Cheng Tang , China
Weerachart Tangchirapat , Thailand
Xiixin Tao, China
Piergiorgio Tataranni , Italy
Elisabete Teixeira , Portugal
Jorge Iván Tobón , Colombia
Jing-Zhong Tong, China
Francesco Trentadue , Italy
Antonello Troncone, Italy
Majbah Uddin , USA
Tariq Umar , United Kingdom
Muahmmad Usman, United Kingdom
Muhammad Usman , Pakistan
Mucteba Uysal , Turkey

Ilaria Venanzi , Italy
Castorina S. Vieira , Portugal
Valeria Vignali , Italy
Claudia Vitone , Italy
Liwei WEN , China
Chunfeng Wan , China
Hua-Ping Wan, China
Roman Wan-Wendner , Austria
Chaohui Wang , China
Hao Wang , USA
Shiming Wang , China
Wayne Yu Wang , United Kingdom
Wen-Da Wang, China
Xing Wang , China
Xiuling Wang , China
Zhenjun Wang , China
Xin-Jiang Wei , China
Tao Wen , China
Weiping Wen , China
Lei Weng , China
Chao Wu , United Kingdom
Jiangyu Wu, China
Wangjie Wu , China
Wenbing Wu , China
Zhixing Xiao, China
Gang Xu, China
Jian Xu , China
Panpan , China
Rongchao Xu , China
HE YONGLIANG, China
Michael Yam, Hong Kong
Hailu Yang , China
Xu-Xu Yang , China
Hui Yao , China
Xinyu Ye , China
Zhoujing Ye, China
Gürol Yildirim , Turkey
Dawei Yin , China
Doo-Yeol Yoo , Republic of Korea
Zhanping You , USA
Afshar A. Yousefi , Iran
Xinbao Yu , USA
Dongdong Yuan , China
Geun Y. Yun , Republic of Korea

Hyun-Do Yun , Republic of Korea
Cemal YİĞİT , Turkey
Paolo Zampieri, Italy
Giulio Zani , Italy
Mariano Angelo Zanini , Italy
Zhixiong Zeng , Hong Kong
Mustafa Zeybek, Turkey
Henglong Zhang , China
Jiupeng Zhang, China
Tingting Zhang , China
Zengping Zhang, China
Zetian Zhang , China
Zhigang Zhang , China
Zhipeng Zhao , Japan
Jun Zhao , China
Annan Zhou , Australia
Jia-wen Zhou , China
Hai-Tao Zhu , China
Peng Zhu , China
QuanJie Zhu , China
Wenjun Zhu , China
Marco Zucca, Italy
Haoran Zuo, Australia
Junqing Zuo , China
Robert Černý , Czech Republic
Süleyman İpek , Turkey

Contents

Analysis of the Customer Churn Prediction Project in the Hotel Industry Based on Text Mining and the Random Forest Algorithm

Leila Taherkhani, Amir Daneshvar , Hossein Amoozad Khalili , and Mohamad Reza Sanaei
Research Article (8 pages), Article ID 6029121, Volume 2023 (2023)

Implementation of an Advanced Macroelement Beam Model under Moving Load (Case Study: Iranian Railroad Projects)

Hamid Reza Vaziri , Mohammad Reza Mansoori , Fereydoon Arbabi, and Armin Aziminejad 
Research Article (16 pages), Article ID 9689218, Volume 2023 (2023)

Research Article

Analysis of the Customer Churn Prediction Project in the Hotel Industry Based on Text Mining and the Random Forest Algorithm

Leila Taherkhani,¹ Amir Daneshvar ,² Hossein Amoozad Khalili ,³ and Mohamad Reza Sanaei⁴

¹Department of Information Technology Management, Science and Research Branch, Islamic Azad University, Tehran, Iran

²Department of Industrial Management, Science and Research Branch, Islamic Azad University, Tehran, Iran

³Department of Industrial Engineering, Sari Branch, Islamic Azad University, Sari, Iran

⁴Department of Information and Technology Management, College of Management and Economics, Qazvin Branch, Islamic Azad University, Qazvin, Iran

Correspondence should be addressed to Amir Daneshvar; a_daneshvar@iauec.ac.ir

Received 12 December 2022; Revised 17 June 2023; Accepted 10 August 2023; Published 24 August 2023

Academic Editor: Afshar A. Yousefi

Copyright © 2023 Leila Taherkhani et al. This is an open access article distributed under the Creative Commons Attribution License, which permits unrestricted use, distribution, and reproduction in any medium, provided the original work is properly cited.

The ability of hotels to differentiate themselves from competitors and continue to operate profitably depends on their ability to retain their customers by building long-term and permanent customer relationships. Technological developments in recent years have made it possible for companies to predict their customers' behavior by accessing their opinions faster and preventing them from churning. Managing customer churn prediction projects has become an important issue today, especially in the hotel industry. Therefore, this research seeks to analyze projects that predict the churn of hotel customers to provide a model to help hotel managers in this field. In this research, an approach based on text mining on customers' comments in the Persian language is presented, which uses the random forest algorithm for classification that was considered the most effective method to solve this problem. In this model, to increase the efficiency of the proposed method in compare with existing works, the gravitational search algorithm was used to select the useful features, and the differential evolution algorithm was used to adjust the parameters of the classification method. The dataset of this research is the collected data from the customer database on social networks and hotels' websites, especially the hotels on Kish Island in Iran. The results of this research showed that after the implementation of the preprocessing operations, the method of adjusting the parameters and removing the unimportant features, the model's accuracy increased significantly. The precision, recall, F1, and accuracy criteria were 0.77, 0.76, 0.76, and 0.77, respectively.

1. Introduction

Customer churn prediction (CCP) is one of the most critical problems for a healthy growing business, regardless of size. CCP allows professionals to estimate the number of customers who abandon a company's product or service in a given period of time and take the necessary actions to retain them. In various markets, customers can quickly terminate their subscriptions with suppliers and switch to competing organizations for increased service quality and lower prices [1, 2]. Accurately predicting customer churn can effectively help customer retention and economical marketing activities

and, therefore, can lead to significant savings for suppliers. Extensive research has been done in this field in sectors such as telecommunications and the hotel industry is no exception.

Online customer feedback tools enable organizations to generate and share content and feedback through social media. According to the report SiteMinder [3], 96% of hotel guests consider users' comments essential when searching for a hotel, and 79% read between 6 and 12 users' comments before making a decision. Therefore, reviews of users' comments affect hotel guests' decision-making and hotels' performance [4], and the value of user-generated content should be further investigated. This issue provides various opportunities

for both companies and users. For example, in the hotel industry, there is a growing interest in analyzing the opinions of different guests and finding hidden patterns or influencing factors [5, 6]. Therefore, it is imperative to check customer churn based on text mining in the hotel industry. At present, the literature on big data mainly focuses on techniques such as sentiment analysis, latent Dirichlet allocation, regression modeling, and others. Despite these valuable contributions, new methods to understand the hidden concepts in unstructured data for different hospitality fields are needed. While there have been many studies and research projects on big data and business analysis, few research studies have investigated the actual content produced by customers on social media and the factors affecting their experience and flow of customers. In addition, how to use analytics tools to analyze user-generated content has not been widely studied, so this research has been addressed how to combine techniques such as text mining and random forest algorithm for CCP in the hotel industry.

The structure of the article is as follows: in the second part, we examine the background of the research. In the third part, we present the proposed system and research methodology. In the fourth part, we describe the dataset and the tools used for data analysis. In the fifth section, we present the results of data analysis in the form of tables and graphs. In the sixth part, we give explanations about managerial insights and practical implications, and in the seventh and final part of the article, we will have conclusions and suggestions.

2. Literature Review

During the last decade, CCP has received increasing attention to survive in a competitive and global market [7]. Companies should strive for models that can accurately identify potential churn customers. This issue becomes more critical with the development of information technology. During the last decade, many experts and academics were interested in this topic and paid attention to it. Several methods presented in recent years will be reviewed below. The primary purpose of the study conducted by Dursun Cengizci [8] was to predict the customers' behavior of a hotel business using machine learning methods in its customer database. In this context, CCP was applied using the data of regular customers of a hotel chain in Antalya, which has three five-star hotels, and logistic regression and random forest algorithms were compared. According to the findings of this study, the random forest algorithm performs better. It could accurately predict 80% (area under the curve (AUC) 0.80) of repeat customers who were likely to leave within the next 3 years.

To investigate the causes of customer churn in Ctrip agency, Zhao et al. [9] used the current and potential value in the customer value system to determine the influencing factors. This research used the random forest algorithm to build the Ctrip CCP model, and the confusion matrix and receiver operating characteristic (ROC) curve were used to evaluate the model. The results showed that the random forest algorithm can better solve the classification problem of CCP, and the accuracy of the prediction model reached 94%. In the research of Han [10], the customer churn of hotel

reservation websites has been investigated in China. In this research, logistic regression and random forest algorithms were used to identify the characteristics that affect customer churn. The experimental evaluation of this research showed that the model had an accuracy of 78.9%.

In the research of Yang [11], Ctrip hotel customers' data were analyzed. First, a supervised feature selection method was used to select features that had a significant impact on customer churn. Then the best model was chosen from logistic regression, support vector machine, decision tree, random forest, GBDT, XGBoost, and LightGBM. A subset of optimal models was selected, and then integration of the optimal models was performed. Experimental results showed that multi-model fusion has higher accuracy and stability.

The study done by Christodoulou et al. [12] solved the problem of revisiting tourists from the point of view of big data analysis. The applied method used topic modeling, word embedding, XGBoost, and random forest classification algorithms. The data were collected from TripAdvisor. Topics were generated using STM topic modeling and information retrieval using Word2vec. The learned model achieved satisfactory performance. The XGBoost classification model achieved a prediction accuracy of 84% and an AUC of 90% for the study of tourists revisiting two to three-star hotels and a prediction accuracy of 89% and an AUC of 90% for four to five-star hotels. The goal of research by Gartvall and Skånshagen [13] was to predict hotel cancellations using machine learning and analyze the factors that have the most significant impact. The data were provided by a hotel in the Gothenburg area. The machine learning algorithms used in the thesis were random forest, XGBoost, and logistic regression. The main findings of this research showed that random forest is the best-performing model in hotel data, with an accuracy of nearly 80%. In the study conducted by Oh et al. [14], deep learning techniques were combined with expectation-confirmation theory to predict customer satisfaction with hotel services. The results showed that this model achieved an accuracy of 83.54%.

In the article by Nagaraju and Vijaya [15], a method was developed to identify the prediction of customer churn in the insurance sector using meta-heuristics and bagging and boosting techniques. In this research, an approach based on meta-heuristic feature selection was proposed to identify effective features. In this study, the combination of firefly enhanced with boosting group classifiers achieved the highest accuracy of 97.12. In the research conducted by Lalwani et al. [16], the prediction of customer churn in the telecommunications industry was made by using machine learning techniques. After data preprocessing, feature selection was made using the gravity search algorithm. In the prediction process, the most common models, including logistic regression, naive Bayes, support vector machine, random forest, and decision trees, were used. K-fold cross-validation was used to adjust hyperparameters and prevent overfitting. The results showed that AdaBoost and XGBoost classifiers have the highest accuracy of 81.71% and 80.8%, respectively. In the research done by Wu et al. [17], a tree-based mechanism was presented that considers temporal and behavioral information separately. Extensive tests in this research

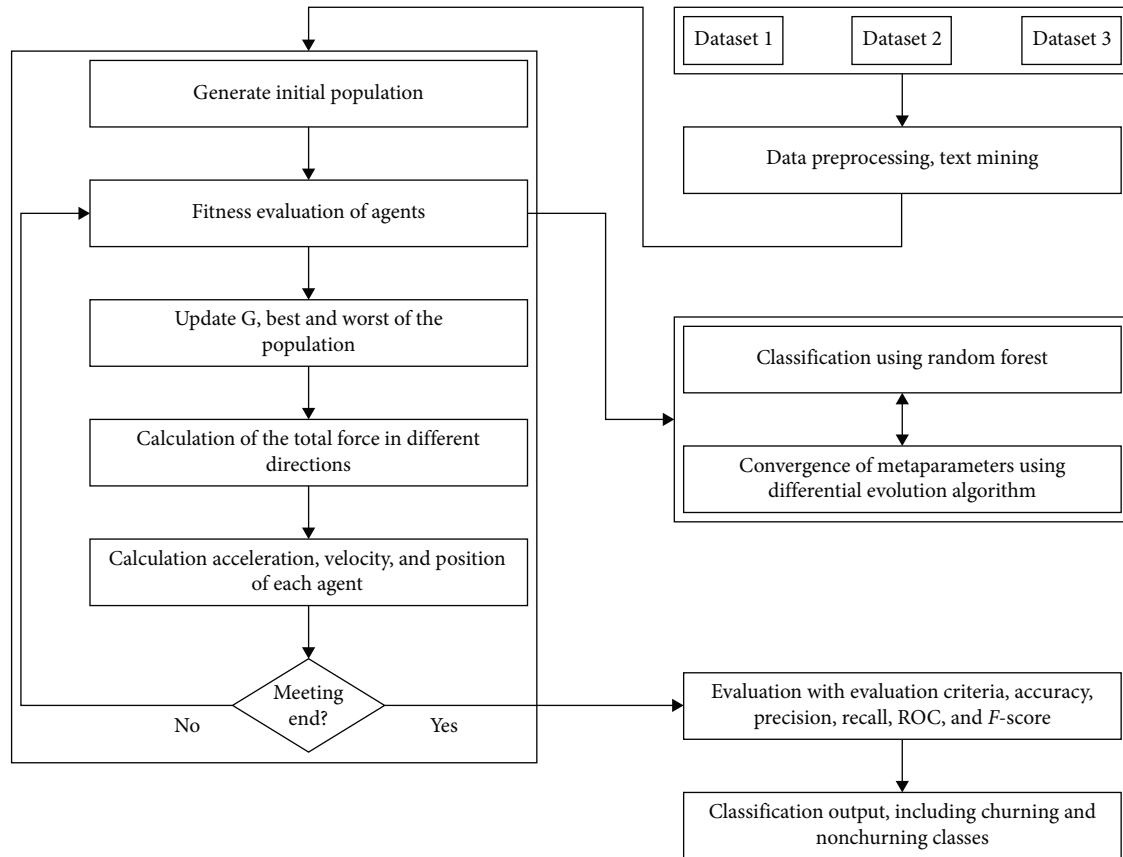


FIGURE 1: Proposed system.

showed that the proposed system achieved an F score of 82.72 and an AUC of 93.75.

Based on the background of the research, the previous studies in this field were mainly on the English language, and less attention was paid to other languages. Therefore, in this research, Persian data available on online platforms have been used, so the purpose of this research is to address this gap and predict customer churn using analytics of user-generated online Persian content. Also, this research intends to analyze the text content produced by customers through combining text mining methods and random forest algorithms and develop a model for CCP in the hotel industry.

The merits of the proposed method have listed as follows:

- (i) We have applied the combined techniques, gravitational search algorithm to perform feature selection, and differential evolution algorithm to adjust the parameters of the classification method. Then we have compared those with the proposed method.
- (ii) As the considered dataset includes users' online comments in the Persian language, we have applied text mining techniques for preprocessing of data, such as case folding, tokenization, stop-words, stemming, and term frequency—inverse document frequency (TF-IDF).
- (iii) We have applied some of the famous machine learning techniques for classification, which are used for

predictions like gradient boosting classifier, naïve Bayes, decision tree, and KNN. Finally, we have compared those with the proposed classification method.

- (iv) Then we have evaluated the algorithms using the confusion matrix and ROC, which have been mentioned in the form of figures and tables, in order to compare which algorithm performs best for this purpose.

Authors' contribution is using the gravitational search algorithm to select the useful features and combining it with the differential evolution algorithm to adjust the parameters of the classification method. The random forest algorithm was considered to this purpose. Then we evaluated the results through the confusion matrix and ROC, which have been mentioned in the form of figures and tables in order to compare which algorithm performs best for this purpose.

3. Proposed System

The proposed system in this research uses a combination of random forest, gravitational search algorithms, and differential evolution algorithms to predict customer churn. The diagram of the proposed system is shown in Figure 1. The details of this method are mentioned below. The reason for choosing the random forest method for learning the proposed system is the proper performance of this method compared to other machine learning methods in solving the research problem. The proof is provided in Section 5.

TABLE 1: Pseudo code of the differential evolution algorithm.

Pseudo code of differential evolution algorithm
Initial population with randomly generated individuals
Fitness evaluation of all individuals in the population
While the final conditions are not met,
Create the mutant vectors using the mutation strategy
Create trial vectors by combining noisy vectors with parent vectors
Evaluate trial vectors with their fitness values
Select winning vectors as individuals in a new generation
End while

As shown in Figure 1, first, the process of text mining and data preprocessing is done. In this section, operations like case folding, tokenization, stop-words, stemming, and TF-IDF are performed on the primary text data. Each of them is described below. To increase the efficiency of the proposed system, the selection of effective features in this research is made by the gravitational search algorithm. The main reason for using the feature selection method is to identify essential variables to reduce data dimensions and increase classification accuracy. A large number of predictive variables leads to a decrease in model accuracy. In this research, by implementing the gravity search algorithm, it is determined which features are valuable for solving the problem of predicting customer churn in the hotel industry.

Another important issue in obtaining proper performance from classification techniques is the correct setting of their parameters. The importance of the parameters of each learning model and problem-solving method, especially artificial intelligence methods that have been created to simplify problem-solving, is inevitable. The optimal values of these parameters, which generally depend on the characteristics of the problem, have a significant impact on the performance of the mentioned methods and a better search of the solution space. The random forest method has been increasingly used in various sciences and has been more successful than other existing methods in many fields. However, this method, like other learning models, is known to be sensitive to its parameters, and determining the appropriate combination of parameters has a significant impact on the final implementation of the algorithm and the results. Considering the challenge of determining the best values of the parameters, in this research, the differential evolution algorithm is also used to adjust the parameters of the random forest.

3.1. Data Preprocessing. The first section of the proposed method is text preprocessing. In this order, the texts are tokenized first; then, they enter the stage of removing stop words. At this stage, words that are repeated a lot in every document and do not have any meaning will be removed from the document. In the Case Folding step, all words are considered the same in terms of uppercase or lowercase letters. This step is done so that if a word is repeated several times with the same form but with different uppercase and lowercase letters, it is considered once in the modeling [18].

The next stage in the preprocessing step is stemming. The purpose of this stage is to harmonize the form of the

words in the documents. With the help of stemming methods, words that are similar in terms of concept and differ from each other only in appearance are placed in one group and are considered features [19]. In the next stage, the goal is to find the appropriate weight of each word according to the TF-IDF weighting methods. The TF-IDF method is a standard weighting method in text mining studies that assigns the right weight to a word based on the number of repetitions of that word in each document and the number of repetitions in all documents and is calculated from Equation (1). In this regard, t_k refers to the k th word, d_i refers to the i th document, N refers to the total number of existing documents, and d_k refers to the number of documents with the term t_k [20].

$$\text{TF-IDF}(t_k, d_i) = \text{TF}(t_k, d_i) \times \log\left(\frac{N}{d_k}\right). \quad (1)$$

3.2. Classification Model, Random Forest. The random forest method was presented by Breiman [21] as a new development method for decision trees. The general principles of ensemble training techniques are based on the assumption that their accuracy is higher than that of other singular training algorithms. Because it is a combination of several prediction models. It is more accurate than a single model and reduces existing weaknesses [21]. Several decision trees are used in this algorithm. A subset of data is given to each tree. These trees can make decisions and build their classification model with this subset of data [22]. The random forest algorithm is currently one of the best learning algorithms, and due to its good performance in solving the problem of customer churn, it was chosen for classification in this research.

3.3. Differential Evolution Algorithm. The differential evolution algorithm is presented to overcome the primary defect of the genetic algorithm, i.e., the lack of local search. The main difference between the genetic algorithm and the differential evolution algorithm is in the order of the mutation and recombination operators, as well as how the selection operator works in this algorithm. This algorithm uses a differential operator to generate new answers, which causes the exchange of information between members of the population. One of the advantages of this algorithm is having a memory that keeps the information about suitable answers in the current population. The pseudo-code of the differential evolution algorithm is presented in Table 1 [23].

3.4. Gravitational Search Algorithm. The gravitational search algorithm is a population-based and iteration-based stochastic

TABLE 2: Pseudo code of gravitational search algorithm.

Pseudo code of the gravitational search algorithm
Search space identification, initialization of parameters
Random initialization of agents.
While the final conditions are not met, do the following steps:
Fitness evaluation of agents
Update $G(t)$, $best(t)$, $worst(t)$ and $Mi(t)$ for $i = 1, 2, \dots, N$.
Calculation of the total force in different directions
Calculation of acceleration and velocity
Update the position of each agent.
Returning the best solution found.
End While

TABLE 3: Comparison of the impact of feature selection and parameter adjustment mechanism in the proposed system.

Methods	Precision	Recall	F1	Accuracy
Random forest + gravitational search algorithm for feature selection	0.75	0.75	0.76	0.76
Random forest + differential evolution algorithm for parameters adjustment	0.74	0.75	0.76	0.74
Proposed method	0.77	0.76	0.76	0.77

meta-heuristic algorithm. This algorithm is inspired by nature to solve continuous optimization problems. The main idea of this algorithm is to simulate Newton's law of gravity and laws of motion on a population of masses in a constant n -dimensional space. In this algorithm, agents are considered objects, and their performance depends on their mass. Objects attract each other with the force of gravity, which causes the general movement of all objects toward objects with a heavier mass. Heavy masses represent better solutions and move slower than lighter masses. The pseudo-code of the gravitational search algorithm is presented in Table 2 [24].

4. Tools and Datasets

The information for this research was obtained from the customers' databases on social networks and hotels' websites, especially the hotels on Kish Island, from five-star to three-star hotels, and was collected in the form of textual content produced by customers. This dataset has more than 6,000 records and is in the Persian language. Among themes, 2,374 cases belong to customers who may churn, and 3,626 cases are related to nonchurning customers. Considering that the collection of users' comments is the first step of the desired implementation in this research, the comments of customers of Persian websites are first extracted with the help of the Python programming language. In the following, the facilities provided by the Python language were used for preprocessing, preparation of comments, and modeling.

5. Results

The results of this study are examined in this section. As already mentioned, the information for this research was obtained from the customers' databases on social networks and the websites of Kish Island hotels from five stars to three stars. It was collected in the form of text comments produced

by customers. This dataset has more than 6,000 records in the Persian language. Among them, 2,374 cases belong to customers who may churn, and 3,626 cases are related to nonchurning customers. In the first part of the evaluation of the results, an experiment was designed to check the effectiveness of the feature selection mechanisms and the parameter adjustment mechanisms. In this section, in the first case, the results of the proposed system are evaluated only with the feature selection mechanism. The best possible parameters are selected by the gravitational search algorithm. In addition, in this mode, the parameters of the random forest are chosen manually. In the second case, the results of the proposed system are evaluated only by the parameter adjustment mechanism. So, in this section, all the features of the dataset are used to solve the problem, and the differential evolution algorithm is used to adjust the parameters of the random forest.

The results of each mode are shown in Table 3 and were compared in terms of accuracy, recall, F1, and precision. For a better comparison, in Figure 2, the results were shown with the help of graphs. According to the results of this test, the feature selection mechanism has a more significant effect on improving the performance of the proposed system.

In the next experiment, in addition to the proposed system, several basic machine learning methods were applied to the dataset to check the proposed system's performance. Therefore, the methods of random forest, gradient boosting classifier, naive Bayes, decision tree, and KNN were applied to solve the customer churn problem in the hotel industry. The results from each of the methods are in Table 4. Methods were compared, according to precision, recall, F1, and accuracy criteria. Figures 3–6 compare the results obtained from the mentioned methods in different ways.

As shown in these figures, the proposed system of this research has performed better than other methods in the precision, F1, and accuracy criteria with a big difference.

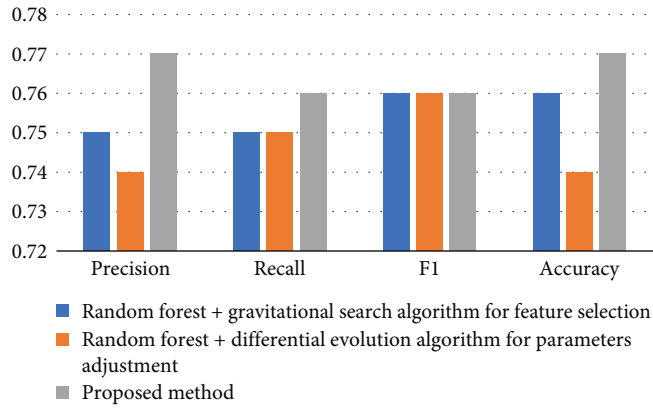


FIGURE 2: Comparison of the impact of feature selection and parameter adjustment mechanism in the proposed system.

TABLE 4: Performance comparison of random forest, gradient boosting classifier, naive Bayes, decision tree, KNN methods, and the proposed system.

Methods	Precision	Recall	F1	Accuracy
Random forest	0.73	0.78	0.75	0.74
Gradient boosting classifier	0.74	0.74	0.74	0.74
Naive Bayes	0.76	0.71	0.73	0.74
Decision tree	0.68	0.66	0.67	0.68
KNN	0.69	0.65	0.67	0.68
Proposed method	0.77	0.76	0.76	0.77

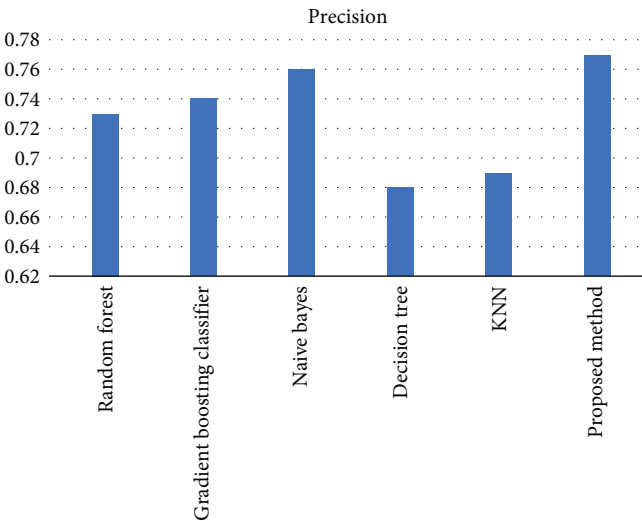


FIGURE 3: Comparison of the precision of random forest, gradient boosting classifier, naive Bayes, decision tree, KNN methods, and the proposed system.

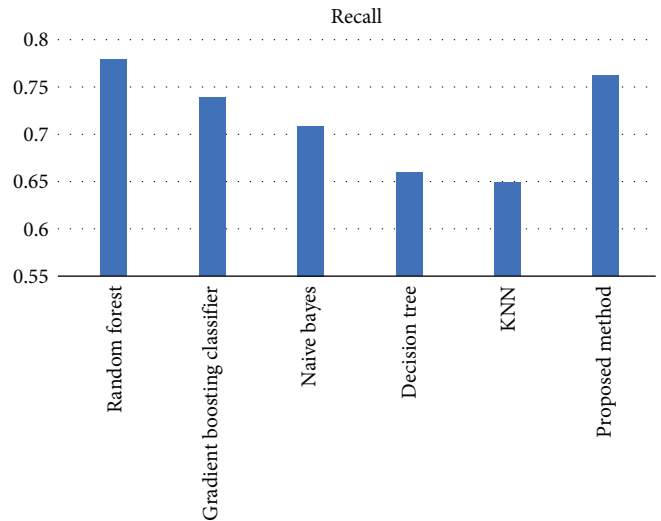


FIGURE 4: Comparison of recall of random forest, gradient boosting classifier, naive Bayes, decision tree, KNN methods, and the proposed system.

The primary random forest method has been better than the proposed method only in the recall criterion. However, this difference is slight, and due to the superiority of the proposed method in the other three criteria, it can be ignored. After the proposed system, among the basic methods, the random

forest method had the best performance, and this issue itself indicates the appropriate choice of classification method in the proposed system. The primary random forest method has performed better than other basic methods regarding recall, F1, and accuracy. Only the naive Bayes method has

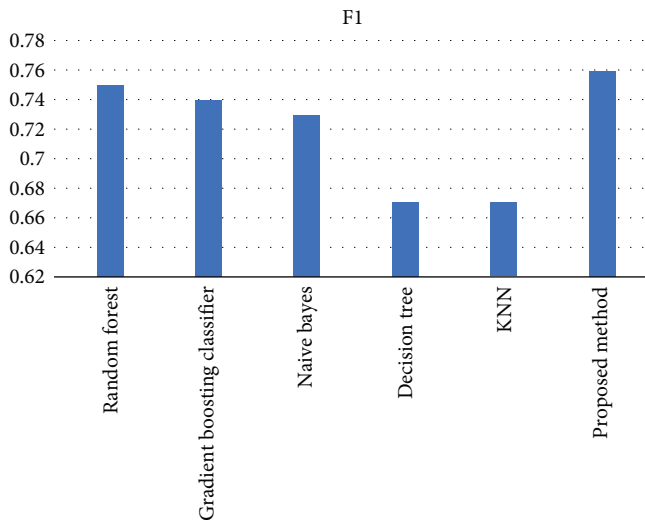


FIGURE 5: Comparison of F1 of random forest, gradient boosting classifier, naive Bayes, decision tree, KNN methods, and the proposed system.

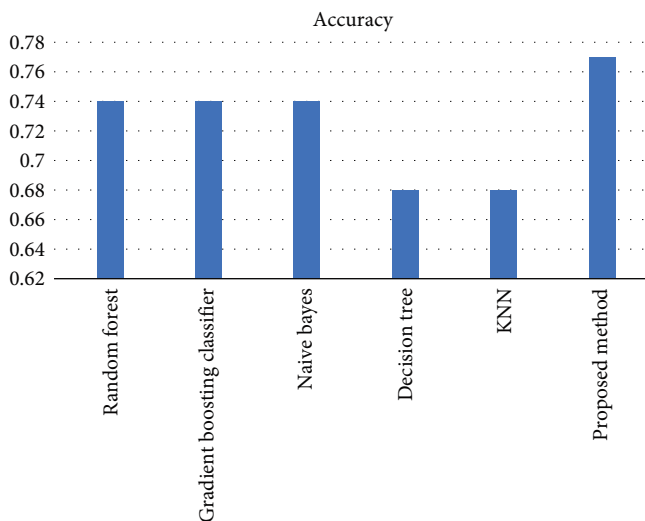


FIGURE 6: Comparison of the accuracy of random forest, gradient boosting classifier, naive Bayes, decision tree, KNN methods, and the proposed system.

served better than the primary random forest method in the precision criterion.

6. Managerial Insights and Practical Implications

By using the method presented in this research, it is possible to achieve reasonable accuracy in predicting the loss of customers. Therefore, the managers of the hotel industry, using the model presented in this research, should identify customer churn early and plan to solve the existing problems. By applying the model introduced in this research to the Persian dataset, it is possible to find the factors influencing the churn of customers. By having these components, the

management of the relevant industry can focus on improving the services that lead to customer churn.

The solution proposed in this research can be applied to all kinds of Persian texts for different industries. Using this method and according to the optimizations, we can expect to achieve the appropriate accuracy for predicting customer churn.

7. Conclusions and Outlook

In this research, a hybrid approach based on text mining, random forest, the gravity search algorithm, and differential evolution is presented to solve the problem of predicting customer churn in the hotel industry. The proposed model helps to extract and review the key performance indicators from the massive volume of comments from hotel customers so that the decision-making process can be done more effectively. The following are the findings of the research:

- (1) The results of the research and comparisons showed that the proposed system of this research has a good performance compared to the compared methods and has reached an accuracy difference of 0.03.
- (2) The proposed method was applied to the set of opinions of hotel customers on Kish Island and the precision, recall, F1, and accuracy criteria; the results were 0.77, 0.76, 0.76, and 0.77, respectively.
- (3) One of the reasons for the superiority of the proposed system is the selection of the random forest method, which, according to the obtained results, has performed better than other basic methods to solve this problem. One of the reasons for the high accuracy of the proposed model compared to the other methods is the feature selection method using the gravity search algorithm. The proposed system's importance of each extracted feature is checked to solve the problem. This method leads to better training of the model by selecting a subset of essential features, thus increasing the model's accuracy.
- (4) The random forest parameter adjustment mechanism using the differential evolution method improves the performance of the random forest method.
- (5) According to the tests, the feature selection process has a more significant impact on system efficiency than the parameter setting and is considered an essential part of problem-solving.

This research, like other research, has limitations. Part of the limitations of the present research are related to the collected dataset, among which the lack of Persian text data in this field and the exclusiveness of the data to several specific hotels can be mentioned.

As a suggestion for the future, the proposed model can be implemented in a cloud-based environment or the Internet of Things to predict travel planning and so on. In addition, ensemble methods can increase the final accuracy of the system by combining the advantages of machine learning techniques.

Data Availability

Data supporting this research article are available from the corresponding author or first author upon reasonable request.

Conflicts of Interest

The authors declare that they have no conflicts of interest.

References

- [1] Y. Li, B. Hou, Y. Wu, D. Zhao, A. Xie, and P. Zou, "Giant fight: customer churn prediction in traditional broadcast industry," *Journal of Business Research*, vol. 131, pp. 630–639, 2021.
- [2] J. Uthayakumar, N. Metawa, K. Shankar, and S. K. Lakshmanaprabu, "Financial crisis prediction model using ant colony optimization," *International Journal of Information Management*, vol. 50, pp. 538–556, 2020.
- [3] SiteMinder, "How to influence travelers: why reviews are the golden egg at your hotel," 2017, <https://www.siteminder.com/r/marketing/hotel-online-reviews/influence-travellers-reviews-hotel>.
- [4] P. Bligh and D. Turk, *CRM Unplugged: Releasing CRM's Strategic Value*, Wiley, Hoboken, NJ, USA, 2004.
- [5] M. Lee, M. Jeong, and J. Lee, "Roles of negative emotions in customers' perceived helpfulness of hotel reviews on a user-generated review website: a text mining approach," *International Journal of Contemporary Hospitality Management*, vol. 29, no. 2, pp. 762–783, 2017.
- [6] Z. Xiang, Z. Schwartz, J. H. Gerdes Jr., and M. Uysal, "What can big data and text analytics tell us about hotel guest experience and satisfaction?" *International Journal of Hospitality Management*, vol. 44, pp. 120–130, 2015.
- [7] N. Gordini, "Market-driven management: a critical literature review," *Symphony Emerging Issues in Management*, no. 2, pp. 95–107, 2010.
- [8] A. Dursun Cengizci, "Otel işletmelerinde kayıp müşteri tahminlemesi," 2020, <https://acikbilim.yok.gov.tr/handle/20.500.12812/32494>.
- [9] Z. Zhao, W. Zhou, Z. Qiu, A. Li, and J. Wang, "Research on ctrip customer churn prediction model based on random forest," in *Business Intelligence and Information Technology. BIIT 2021, vol 107 of Lecture Notes on Data Engineering and Communications Technologies*, A. E. Hassanien, Y. Xu, Z. Zhao, S. Mohammed, and Z. Fan, Eds., pp. 511–523, Springer, Cham, 2021.
- [10] S. Han, "A study on a predictive model of customer defection in a hotel reservation website," in *MATEC Web of Conferences*, vol. 228, p. 1009, EDP Sciences, 2018.
- [11] W. Yang, "Research on early warning of customer churn based on mutual information and integrated learning—taking ctrip as an example," *Academic Journal of Computing & Information Science*, vol. 5, no. 3, pp. 785–800, 2022.
- [12] E. Christodoulou, A. Gregoriades, M. Pampaka et al., "Application of classification and Word Embedding Techniques to Evaluate Tourists' Hotel-revisit Intention," in *Proceedings of the 23rd International Conference on Enterprise Information Systems - Volume 1: ICEIS*, pp. 216–223, SciTePress, 2021.
- [13] E. Gartvall and O. Skånshagen, "Predicting hotel cancellations using machine learning," 2022, https://gupea.ub.gu.se/bitstream/handle/2077/70742/gupea_2077_70742_1.pdf?sequence=1.
- [14] S. Oh, H. Ji, J. Kim, E. Park, and A. P. del Pobil, "Deep learning model based on expectation-confirmation theory to predict customer satisfaction in hospitality service," *Information Technology & Tourism*, vol. 24, no. 1, pp. 109–126, 2022.
- [15] J. Nagaraju and J. Vijaya, "Boost customer churn prediction in the insurance industry using meta-heuristic models," *International Journal of Information Technology*, vol. 14, pp. 2619–2631, 2022.
- [16] P. Lalwani, M. K. Mishra, J. S. Chadha, and P. Sethi, "Customer churn prediction system: a machine learning approach," *Computing*, vol. 104, pp. 271–294, 2022.
- [17] X. Wu, P. Li, M. Zhao, Y. Liu, R. G. Crespo, and E. Herrera-Viedma, "Customer churn prediction for web browsers," *Expert Systems with Applications*, vol. 209, pp. 118–177, 2022.
- [18] C. C. Aggarwal and C. Zhai, *Mining Text Data*, Springer, Boston, MA, USA, 2012.
- [19] C. Ramasubramanian and R. Ramya, "Effective pre-processing activities in text mining using improved porter's stemming algorithm," *International Journal of Advanced Research in Computer and Communication*, vol. 2, no. 12, pp. 4536–4538, 2013.
- [20] S. M. Weiss, N. Indurkha, and T. Zhang, *Fundamentals of Predictive Text Mining*, Springer, London, 2010.
- [21] L. Breiman, "Random forests," *Machine Learning*, vol. 45, pp. 5–32, 2001.
- [22] K. Senagi, N. Jouandeau, and P. Kamoni, "Using parallel Random Forest classifier in predicting land suitability for crop production," *Journal of Agricultural Informatics*, vol. 8, no. 3, pp. 23–32, 2017.
- [23] M. Leon and N. Xiong, "Investigation of mutation strategies in differential evolution for solving global optimization problems," in *International conference on artificial intelligence and soft computing*, pp. 372–383, Springer, Cham, 2014.
- [24] E. Rashedi, H. Nezamabadi-Pour, and S. Saryazdi, "GSA: a gravitational search algorithm," *Information Sciences*, vol. 179, no. 13, pp. 2232–2248, 2009.

Research Article

Implementation of an Advanced Macroelement Beam Model under Moving Load (Case Study: Iranian Railroad Projects)

Hamid Reza Vaziri ¹, Mohammad Reza Mansoori ¹, Fereydoon Arbabi,²
and Armin Aziminejad ¹

¹Department of Civil Engineering, Science and Research Branch, Islamic Azad University, Tehran, Iran

²Department of Civil Engineering, Michigan Technological University, Houghton, MI, USA

Correspondence should be addressed to Mohammad Reza Mansoori; m.mansoori@srbiau.ac.ir

Received 20 September 2022; Revised 2 December 2022; Accepted 24 March 2023; Published 26 April 2023

Academic Editor: Reza Lotfi

Copyright © 2023 Hamid Reza Vaziri et al. This is an open access article distributed under the Creative Commons Attribution License, which permits unrestricted use, distribution, and reproduction in any medium, provided the original work is properly cited.

This study aims to present a new three-dimensional moving macroelement for the numerical analysis of beam on the elastic foundation under moving loads as a railroad track vibration. Our research is based on a case study conducted in Iranian Railroad Projects. Due to involving a large number of elements, vibration analysis of beams as railroad tracks with standard three-dimensional elements is time-consuming. Two approaches are used and combined in this research to improve analysis of realistic models. The former is to use a macroelement with a number of degrees of freedom that can be used in lieu of standard three-dimensional elements. The latter is to use moving elements to ensure that the loads do not approach the boundaries of the model, thus leading to boundary errors. Accordingly, the moving element was formulated at different velocities to allow correct evaluation of the trains' acceleration and deceleration effect. The analysis is based on a linear model. Examples with different number of elements and boundary conditions were included to evaluate the effects of the track parameters. One important aspect of the formulation is the asymmetric nature of stiffness and damping matrices due to the effects of velocity and the moving load. In the moving element method, with a sufficient number of elements, no end condition effect exists. However, because acceleration may be a more critical parameter than displacement, the number of elements must be determined for acceleration, as well. Our important achievements include formulating the interaction of lateral and torsional degrees of freedom, the possibility of calculating probable warping in the beam due to cross-sectional slenderness both directly and based on introducing a dependent degree of freedom, and also determining the model length based on vibrational acceleration at the end of the model. Besides, reduction of analysis time is a prominent feature of the present model.

1. Introduction

Vibration analysis of railroad tracks as beam models on elastic foundations under moving trains is important for both designing new tracks and operating existing ones. Many studies have examined free and forced vibration of continuous beams as tracks under different loading conditions including trains moving at steady speed and while accelerating and braking, as well as temperature changes and the effects of earthquakes. The focus on trains moving on a track stems from the implications for designing and maintenance [1–6].

Fryba [3] employed a Fourier transform when examining a beam under moving loads. Fryba et al. [4] also studied a beam on a foundation having randomly varying stiffness under a moving force using the finite element technique. Chen and Huang [5] and Anderson et al. [6] studied the track as a beam model under a concentrated load and mass. The newly suggested techniques which appear to be very appropriate for railroad tracks due to moving nature of train loads include the moving coordinate method [7] and its counterpart, the moving element method [8].

The current research is based on studies of moving loads, which are relevant to the vibration of tracks under trains. For

instance, Mathews [9] most recently examined a track under a moving load in the frequency domain. Similar studies have been conducted by Jezequel [10] and Ono and Yamada [11], who modeled the rail as an infinite Euler–Bernoulli beam. Trochanis et al. [12] used a Fourier transform in order to model the rail. Calim [13] studied forced vibration of curved beams on a two-parameter elastic foundation subjected to impulsive loads. He modeled the curved beam by finite elements with two degrees of freedom (DoFs) at each node.

Dai et al. [14] analyzed an efficient numerical study on the dynamic response of a partially filled freight train subject to abrupt braking through the moving element method computationally. Nguyen and Duhamel studied the nonlinear behavior of bars [15] and beams [16] on elastic supports under harmonic moving loads. On the bar element, the velocity was assumed to be constant and linear springs were used to model a Winkler foundation, leading to the equations of motion using moving coordinate. On the beam element, the analysis was conducted under similar loading conditions and both studies were carried out in the time domain. The foundation stiffness was given a nonlinear form to make prediction of soil failure possible.

Nguyen et al. [17] analyzed the effect of a moving mass on a nonlinear foundation. Kouroussi and Verlinden [18] modeled a railroad with lumped masses to study train, track, and foundation interactions. Ferreira and López-Pita [19] studied the maintenance needs of railroad tracks through numerical modeling using Dynavoie to optimize the track designs. The finite element model was also used to consider the dynamic interaction between the train and track and all its components.

Zakeri and Xia [20] modeled the beams having infinite lengths on elastic foundations at the end of their finite element model. They showed the possible boundary conditions' effect on the dynamic response. In order to reduce such effects, the length of the track was chosen so as to minimize the dynamic responses at the end points. Because the acceleration response can propagate farther, it is important to choose a length at which acceleration is negligible at the boundaries.

Sarvestan et al. [21] studied vibration of cracked Timoshenko beams subjected to moving loads. The crack was modeled using two massless springs, leading to the dynamic stiffness matrix of the beam. Their study included both a constant velocity and a constant acceleration of moving loads. Spectral analysis was performed in the frequency domain, and the model used a two-dimensional plate element with two DoFs at each node. Uzzal et al. [22] determined the dynamic response of an Euler–Bernoulli beam subjected to moving loads as well as a moving mass supported on a two-parameter Pasternak foundation using the Fourier transform technique. Beam elements were used to simulate different structures including gas pipelines. Hua et al. [23] evaluated the dynamic behavior of an axially moving beam to study its internal pressure using the finite element method. The studied model consisted of a one-dimensional beam subjected to an internal pressure. The Newmark- β time integration method was adopted to calculate the dynamic responses of the model. Finally, effects

of the internal pressure on the dynamic model of the beam were investigated. Afterwards, Mei et al. [24] studied the dynamic behavior of a long beam on an elastic foundation. A reduced time-varying model and Hamilton's principle were employed in their study. More recently, Jahangiri et al. [25] analyzed an Euler–Bernoulli beam under a moving mass with large oscillations using Galerkin and perturbation methods. They solved the problem in presence of an external harmonic force applied on the moving mass through the perturbation method. Phadke and Jaiswal [26] studied the impact of a nonhomogeneous elastic foundation on dynamic response of railway track. The track was modeled as a long beam on a nonhomogeneous elastic foundation.

Using the finite element method, Forio et al. [27] evaluated a simply supported Euler–Bernoulli elastic beam resting on a homogeneous nonlinear elastic Winkler foundation subjected to a concentrated moving load. The beam was examined at different velocities in order to determine the critical velocity at which large displacements could damage the structural elements. The authors established a relationship between the critical velocity and moving load parameters.

The moving coordinate and moving element methods are appropriate for railroad tracks with moving train loads [7, 8]. The former method provides an advantage of the form of the moving load on the rail element, where it is not necessary to determine the end conditions of the model, and thus the load effects are never experienced at the end point. Since the beam model is infinite, the upstream and downstream ends of the beam model are sufficiently far from the load points to make their effect negligible. This form of modeling is similar to that of pushing the rail under the train that each load point contact remains constant.

Koh et al. [7] showed that, in the moving element method, the elements are conceptual and move under the vehicle while it remains stationary. In this way, the relative movement of the vehicle with respect to the track is demonstrated and the train never reaches the end of the track model. Koh et al. [7] considered both smooth rails as well as corrugated ones. Tran et al. [8] continued this research by including variable velocities. In these studies, common one-dimensional beam elements were used as the moving elements. The governing equations of motion were derived using a Galerkin approach with examples primarily related to displacement in one direction. The examples included moving loads with variable velocities at a constant acceleration.

In the present study, a new macroelement and a moving coordinate system are used to evaluate the dynamic response of a beam model as the track under moving train loads. The model is three-dimensional in nature so that the response can be evaluated by considering the interaction of the displacements in different directions. Because this model can provide accurate and economical solutions, it can be used to evaluate the simultaneous effect of earthquakes and moving trains contemporarily or separately. The model can be used to simulate earthquake and train load as a moving load either simultaneously or separately. It also paves the way to

investigate the interaction of lateral and torsional DoFs in related loading cases.

Although the macroelement [28, 29] and the moving element method [7, 8] have been used by previous researchers, the current article combines the two techniques to provide an efficient means of dealing with infinite domain railroad tracks. The moving element method ensures that the effect of end conditions does not invalidate the results. In modeling the track system, the smooth rail is modeled as an Euler–Bernoulli beam resting on an elastic base. The base is represented by linear springs that can be either continuous or discrete. In numerical examples, continuous springs are generally used. The springs can also be rotational to allow modeling of rotational stiffness. The macroelement requires seven DoFs, six of which for modeling displacement and rotations in a three-dimensional coordinate along with a dependent additional DoF for modeling possible warping of the rail. Besides, due to such gaps in previous studies as follows, the current study seemed to be necessary: (1) lack of accurate modeling of rail bed, (2) impossibility of modeling and accurate investigation of bed damping, and (3) lack of providing a comprehensive model for use in curved and straight beams.

Here, the following basic problems are to be answered:

- (1) Introduction of a comprehensive macroelement model for straight railway lines located on elastic bed.
- (2) What are the limitations of the length of the rail? And what factors the number of model elements in modeling depend on?
- (3) What is the effect of moving load parameters such as speed and acceleration as well as the amount of load on the response of the rail?
- (4) What are the effects of rail interaction in different degrees of freedom?

2. Problem Statement

The symbols used in the equations are defined in Table 1.

2.1. Formulation of Macroelement. The macroelement used in this study was developed by Arbabi et al. [28–33] and proved to be an efficient model for studying unbounded domains such as railroad tracks. The element (Figure 1(a)) has two nodes with seven DoFs at each node. One, u , is related to axial deformation in the x direction, and the lateral deformations v and w are in the vertical and horizontal (y and z) directions, respectively. The rotational deformations about y and z axes are θ_z and θ_y , respectively.

Rotation about the x axis is dominant because it describes the torsional deformation. Its derivative is the warping parameter denoted by β without a subscript. In order to calculate warping, a separate DoF is denoted as β . Figure 1 shows that the parts of the rail section below the head have much thinner sections; therefore, warping can be significant.

Since the foundation provides distributed support for the rails, distributed springs were used to model the foundation. The springs are in the vertical and horizontal directions denoted as k_y and k_z , respectively. Similar springs exist in the x direction to account for the axial stiffness of the track caused by the friction between the traverses and ballast as well as the ballast and the ground. The interaction of the ballast and railroad traverses can also provide rotational resistance against the bending of the rails. The distributed torsional spring, k_t , is provided to account for such resistance. The vertical and horizontal dashpots with coefficients c_y and c_z are provided to address damping of the track.

2.2. Rail Properties. The component properties of the numerical examples considered here are those used in Iranian railroads [34]. The properties of the cross sections of the rails, UIC-60, are presented in Figure 2 [34] and Table 2.

In McGuire et al. [35], warping constant Γ is calculated as follows:

$$\Gamma = \frac{I_y d^2}{4}, \quad (1)$$

where I_y is the second moment of area about the y axis and d is the height of the rail section. For portions of the track where the traverses are placed on concrete slabs, a concrete strength of $f'_c = 400 \text{ kg/cm}^2$ is assumed and modulus of elasticity E_c has been calculated according to the Iranian concrete code. Table 3 lists the stiffness and the dashpot properties of the railroad models.

2.3. Governing Equations for Moving Macroelements. Beams on elastic foundations are used for different engineering problems. Thus, the formulations can be one, two, or three-dimensional. The one-dimensional case under axial deformation is applied for pile-driving as well as for railroad tracks. Because of its simplicity, it is also a good problem for the demonstration of the formulation process. Metrikine and Dieterman [36] modeled a beam on a viscoelastic foundation under a mass moving in the axial direction. They assumed that the mass and the beam are in continuous contact and have a vertical constant force, respectively.

The equation of motion is found by applying the Hamilton principle, after which the coordinates change to a new moving coordinate system. The Hamilton principle leads to

$$\int_{t_1}^{t_2} \delta(K - \Pi) dt + \int_{t_1}^{t_2} \delta W dt = 0, \quad (2)$$

where K is the kinetic energy of the mass, Π denotes the potential energy of the beam and supports, and W is the nonconservative work of damping. The total kinetic energy can be written in terms of the kinetic energy of the moving mass plus the work of the external force.

TABLE 1: Symbol definition.

Symbol	Definition
u, v, w	Axial and lateral deformation in the $x, y,$ and z directions, respectively
$\dot{u}, \dot{v}, \dot{w}$	Axial and lateral velocity in the $x, y,$ and z directions, respectively
$\ddot{u}, \ddot{v}, \ddot{w}$	Axial and lateral acceleration in the $x, y,$ and z directions, respectively
β	Torsion angle around x direction
β'	Warping factor definition
$\bar{k}_x, \bar{k}_y, \bar{k}_z$	Stiffness factor per unit length of the beam in the $x, y,$ and z directions, respectively
k_t	Rotational stiffness factor per unit length of the beam
$\bar{c}_x, \bar{c}_y, \bar{c}_z$	Damping factor per unit length of the beam in the $x, y,$ and z directions, respectively
\bar{c}_t	Rotational damping factor per unit length of the beam
\bar{m}	Mass per unit length of the beam
\bar{J}_m	Rotational mass inertia per unit length of the beam
E	Modulus of elasticity
A	Area section
Γ	Warping factor
K	Kinetic energy
Π	Potential energy
W	Nonconservative works
ρ	Mass density
ε	Strain of beam model
I_x, I_y, I_z	The second moment of area in the $x, y,$ and z directions, respectively
J	Second polar moment of area
h	Distance between shear center and bottom level of the rail
P, q_y, q_z	Moving point load in the $x, y,$ and z directions, respectively
T	Concentrated rotational moment around the x axis

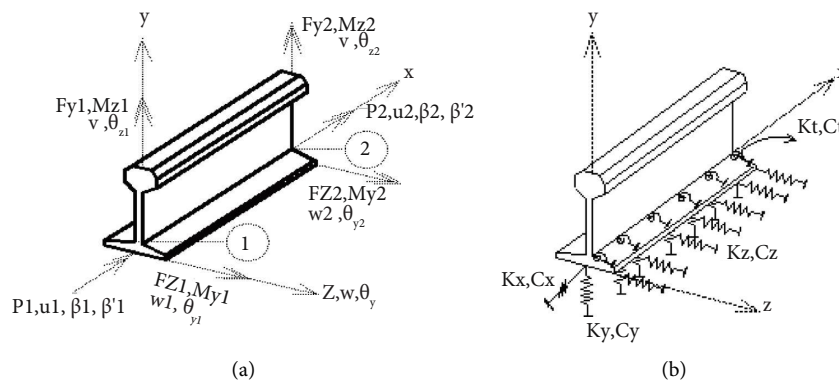


FIGURE 1: Rail macroelement model and DoF definitions [28].

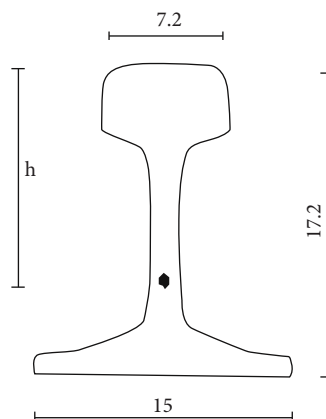


FIGURE 2: UIC-60 rail section (cm) [34].

TABLE 2: Rail section properties.

Definition	Symbol	Value
Weight per unit length	\bar{W}	6034 kg/m
Section area	A	7587 mm ²
Second area moment about z axis	I_z	30.55 × 10 ⁶ mm ⁴
Second area moment about y axis	I_y	5.13 × 10 ⁶ mm ⁴
Modulus of elasticity	E	2 × 10 ⁵ MPa
Weight per unit volume	γ	7.85 ton/m ³
Warping constant [35]	Γ	3.79 × 10 ¹⁰ mm ⁶

TABLE 3: Spring and dashpot properties of models.

Definition	Symbol	Value
Stiffness in y direction	\bar{k}_y	1.00 × 10 ⁷ N/m
Stiffness in z direction	\bar{k}_z	1.67 × 10 ⁶ N/m
Rotational stiffness	\bar{k}_t	4.58 × 10 ⁴ (N·m)/m
Damping factor in y direction	\bar{c}_y	4900 (N·s)/m
Damping factor in z direction	\bar{c}_z	2500 (N·s)/m

2.3.1. *Equilibrium Equation for Axial Deflection.* The Hamilton principle for the axial deformation is defined as follows:

$$\int_{t_1}^{t_2} \delta(K_{\text{axial}} - \Pi_{\text{axial}}) dt + \int_{t_1}^{t_2} \delta W_x dt = 0, \quad (3)$$

in which

$$K_{\text{axial}} = \frac{1}{2} \int_V \rho \dot{u}^2 dV, \quad (4)$$

where K_{axial} is kinetic energy in terms of axial displacement (equations (4) and (5)). By setting the mass per unit length as $\bar{m} = \rho A$ and $dV = Adx$, the last equation would be as follows:

$$W_x = \int_0^l \frac{1}{2} f_{DX} (\delta u)^2 dx \implies \delta W_x = \int_0^l f_{DX} \delta u dx \text{ with } f_{DX} = \bar{c}_x \dot{u}, \quad (8)$$

$$\delta W_x = - \int_0^l \bar{c}_x \dot{u} \delta u dx, \quad (9)$$

where \bar{C}_x is the damping factor per unit length as shown in Figure 1(b). Following variational calculus rules, we get

$$\int_{t_1}^{t_2} \delta \left(\frac{du}{dt} \right) dt = \int_{t_1}^{t_2} \frac{d}{dt} (\delta u) dt. \quad (10)$$

Through integration by parts and assuming that δu is the nonzero variation of the displacement, the statement of the Hamilton principle is

$$K_{\text{axial}} = \frac{1}{2} \int_0^l \bar{m} \dot{u}^2 dV. \quad (5)$$

The potential energy in the axial direction is defined as

$$\Pi_{\text{axial}} = \Pi_{a-i} + \Pi_{a-e} = \frac{1}{2} \int_V E \varepsilon^2 dV + \frac{1}{2} \int_l \bar{k}_x u^2 dx - P \cdot u, \quad (6)$$

where Π_{a-i} is the internal potential energy due to the elastic deformation of the beam and Π_{a-e} is the potential energy of the support due to its stiffness effect and the work of external load on the model. Here, the foundation is modeled as a distributed linear spring in the x direction with stiffness \bar{k}_x per unit length of the beam. Equation (3) converts to

$$\frac{1}{2} \int_0^l \bar{m} \dot{u}^2 dx + \frac{1}{2} \int_0^l EA u'^2 dx + \frac{1}{2} \int_0^l \bar{k}_x u^2 dx + \int_0^l \delta W_x dx = 0, \quad (7)$$

where ε is the axial strain and is equal to the first partial differential of u as $\varepsilon = (\partial u / \partial x) = u'$ and E is the modulus of elasticity of the beam. The nonconservative work of the axial force is

$$\bar{m} \ddot{u} + \bar{c}_x \dot{u} - EA u'' + \bar{k}_x u = p \cdot \delta(x - Vt). \quad (11)$$

2.3.2. *Equilibrium Equation for Vertical Deflection.* In vertical direction y , which is the direction of the applied weight of the train and the locomotive, the process is similar to that in the axial direction. The expression of the Hamilton principle in this case is

$$\int_{t_1}^{t_2} \delta(K_{y\text{-bending}} - \Pi_{y\text{-bending}}) dt + \int_{t_1}^{t_2} \delta W_y dt = 0. \quad (12)$$

The expression for axial strain due to bending as derived according to the strength of materials [37] is

$$\frac{1}{2} \int_{t_1}^{t_2} \int_0^l \delta \left[(m\dot{v}^2) - (EI_z v'' + \bar{k}_y v^2 - q_y v) \right] dx dt + \int_{t_1}^{t_2} \int_0^l \delta(-\bar{c}_y \dot{v} \delta v) dx dt = 0. \quad (13)$$

The following substitutions can be made:

$$\Pi_y = \frac{1}{2} \int_0^l EI_z v'' dx + \frac{1}{2} \int_0^l \bar{k}_y v^2 dx - q_y v \text{ with } v'' = \frac{\partial^2 v}{\partial x^2}. \quad (14)$$

The nonconservative work of the vertical force can be substituted as

$$\delta W_y = - \int_0^l \bar{c}_y \dot{v} \delta v dx, \quad (15)$$

where \bar{C}_y is the vertical damping factor per unit length which accounts for damping of the soil, ballast, and traverses. After integration of the Hamilton principle in equation (12) and by setting the variation to zero, the equilibrium equation for vertical motion becomes

$$\bar{m} \frac{\partial^2 v}{\partial t^2} + \bar{c}_y \frac{\partial v}{\partial t} + \bar{k}_y v + EI_z \frac{\partial^4 v}{\partial x^4} = q_y \cdot \delta(x - Vt). \quad (16)$$

2.3.3. Equilibrium Equation for Lateral (Horizontal) Displacement. In the lateral z direction, the resistance of the ballast against movement of the rail acts at the base of the rail. It is important that the eccentricity of this resisting force with respect to the shear center of the rail section is not

$\varepsilon = -y(\partial^2 v / \partial r^2)$. Having this, the expression of the Hamilton principle is

ignored. The resisting force is assumed to act at the shear center, neglecting the torsional moment induced by lateral resistance. Because this force is important in the investigation of rail overturning, which is common in train derailments, eccentricity has been taken into account and can be set to zero when comparing the results of the form without the effects of the eccentricity. The remaining formulation is similar to the formulation for vertical displacement.

Figure 1(b) shows that the lateral resisting force of the ballast is $\bar{k}_z(w - \beta h)$, where h is the distance between the top of the traverses and the shear center of the rail cross section according to Figure 2, and \bar{k}_z is the lateral stiffness per unit length of the track. Using the same steps as in the derivation of the equilibrium equations in the vertical direction produces the following equation:

$$\bar{m} \frac{\partial^2 w}{\partial t^2} + \bar{c}_z \frac{\partial w}{\partial t} + \bar{k}_z(w - \beta h) + EI_y \frac{\partial^4 w}{\partial x^4} = q_z \cdot \delta(x - Vt). \quad (17)$$

The effect of torsion around the axial x axis has conditions that are similar to the calculation in the z direction. The equilibrium equation for torsion about the axis of the track (x axis) is

$$\bar{J}_m \ddot{\beta} + GJ\beta'' + (\bar{k}_t + \bar{k}_z h^2)\beta + EI\beta^{iv} - \bar{c}_t \dot{\beta} + 2\bar{k}_z h w = T \cdot \delta(x - Vt). \quad (18)$$

In all the formulations, $\delta(x - Vt)$ is a Dirac delta function that shows the effect of the moving load.

2.3.4. Moving Coordinate System. As stated earlier, when modeling a track with a moving train, a prohibitive number or elements may be needed for the track in order to eliminate the boundary effects. This makes the use of common finite elements unworkable. Even with macroelements, practical problems are time-consuming to model on most computers. This can be alleviated by use of moving coordinates and their counterpart moving elements. In this approach, the load remains stationary, but the track moves under the load. The load then will never approach the boundaries to invalidate the results because of the boundary effects.

Consider a fixed Cartesian coordinate system x - y . Assume that the load is at the middle of the track model at point O' , and the coordinate x' - y' at point O' is not fixed but moves at speed V , which is the same as the velocity of the moving load. In addition to eliminating the boundary effects on the critical portion of the track, which is the area of application of the load, additional advantages exist for the moving coordinate system related to unbounded problems. An example is the railroad track in that the location of the load does not change and there is no need to keep track of the element upon which the load is located or to modify its properties. Once the load vector is set, it need not be updated again. In addition, multi-axle loads (trains and locomotives) can be modeled by using appropriate element lengths so that the loads act at the nodes. Referring to Figure 3, the relation

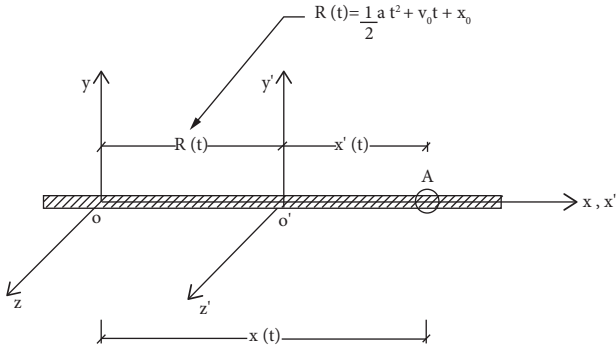


FIGURE 3: Moving coordinates and relationships for Cartesian coordinates.

between the old (fixed) and new (moving) coordinate systems is presented in equations (19) and (20), respectively:

$$\frac{\partial}{\partial t} \longrightarrow \frac{\partial}{\partial t} - B \frac{\partial}{\partial x'(t)}, \quad (19)$$

$$\frac{\partial^2}{\partial t^2} \longrightarrow \frac{\partial^2}{\partial t^2} - a \frac{\partial}{\partial x'(t)} - 2B \frac{\partial^2}{\partial x'(t) \partial t} + B^2 \frac{\partial^2}{\partial x'(t)^2}, \quad (20)$$

where a is the constant acceleration of the load, $B = at + V_0$ in which V_0 is the velocity of the moving load, and t is time. Here, the train motion is considered to have variable velocity but constant acceleration. This allows for the investigation of trains moving at constant speed as well as accelerating and decelerating trains near the stations. For simplicity, this is written as $r = x'(t)$. Equations (12), (17), (18), and (19) in the new coordinate system take the form of equations (21)–(24), respectively:

$$\bar{m} \left(\frac{\partial^2 u}{\partial t^2} - a \frac{\partial u}{\partial t} - 2B \frac{\partial^2 u}{\partial r \partial t} + B^2 \frac{\partial^2 u}{\partial r^2} \right) + \bar{c}_x \left(\frac{\partial u}{\partial t} - B \frac{\partial u}{\partial r} \right) + \bar{k}_x u - EA \frac{\partial^2 u}{\partial r^2} - P \cdot \delta(r + x_0) = 0, \quad (21)$$

$$\bar{m} \left(\frac{\partial^2 v}{\partial t^2} - a \frac{\partial v}{\partial t} - 2B \frac{\partial^2 v}{\partial r \partial t} + B^2 \frac{\partial^2 v}{\partial r^2} \right) + \bar{c}_y \left(\frac{\partial v}{\partial t} - B \frac{\partial v}{\partial r} \right) + \bar{k}_y v - EI_z \frac{\partial^4 v}{\partial r^4} - q_y \cdot \delta(r + x_0) = 0, \quad (22)$$

$$\bar{m} \left(\frac{\partial^2 w}{\partial t^2} - a \frac{\partial w}{\partial t} - 2B \frac{\partial^2 w}{\partial r \partial t} + B^2 \frac{\partial^2 w}{\partial r^2} \right) + \bar{c}_z \left(\frac{\partial w}{\partial t} - B \frac{\partial w}{\partial r} \right) + \bar{k}_z (w - \beta h) - EI_y \frac{\partial^4 w}{\partial r^4} - q_z \cdot \delta(r + x_0) = 0, \quad (23)$$

$$\bar{J}_m \left(\frac{\partial^2 \beta}{\partial t^2} - a \frac{\partial \beta}{\partial t} - 2B \frac{\partial^2 \beta}{\partial r \partial t} + B^2 \frac{\partial^2 \beta}{\partial r^2} \right) + \bar{c}_t \left(\frac{\partial \beta}{\partial t} - B \frac{\partial \beta}{\partial r} \right) + (\bar{k}_t + \bar{k}_z h^2) \beta - EI \frac{\partial^4 \beta}{\partial r^4} - 2\bar{k}_z h w - T \cdot \delta(r + x_0) = 0. \quad (24)$$

2.3.5. Finite Element Formulation. These equations can be cast in finite element form with the standard process. Because the formulations in equations (21)–(24) are in the moving coordinate system, the results would be moving elements. In this case, instead of moving, the load will remain stationary while the elements under it move to produce the relative movement of the track and train. This begins by expressing the displacement of an arbitrary point in terms of nodal displacements by employing the standard shape functions for a beam element as

$$X = \sum NS, \quad (25)$$

where X denotes a vector such as u, v, w, β which is known as the deformation vector. For macroelement deformation, the shape functions are

$$N_u = Nu_{1 \times 14}, N_v = Nv_{1 \times 14}, N_w = Nw_{1 \times 14}, N_\beta = N\beta_{1 \times 14}, \quad (26)$$

where $Nu_{1,1} = x/l$ and $Nu_{1,8} = 1 - x/l$ and the other matrix elements of the shape function for axial deformation are equal to zero. For vertical and lateral deformations, as well as torsion, the shape function is the same:

$$N = [N1 \ N2 \ N3 \ N4], \quad (27)$$

where

$$N1 = \frac{2x^3}{l^3} - \frac{3x^2}{l^2} + 1, \quad (28)$$

$$N2 = \frac{x^3}{l^2} - \frac{2x^2}{l} + x, \quad (29)$$

$$N3 = \frac{2x^3}{l^3} + \frac{3x^2}{l^2}, \quad (30)$$

$$N4 = \frac{x^3}{l^2} - \frac{x^2}{l}. \quad (31)$$

In the macroelement, the degrees of freedom are defined in Figure 1(a), with the shape functions as $Nv_{1,2} = N1$, $Nv_{1,3} = N2$, $Nv_{1,9} = N3$, and $Nv_{1,10} = N4$ as well as $Nw_{1,4} = N1$, $Nw_{1,5} = N2$, $Nw_{1,11} = N3$, and $Nw_{1,12} = N4$. For the torsion DoFs, the elements of shape function matrix can be defined as $N\beta_{1,6} = N1$, $N\beta_{1,7} = N2$, $N\beta_{1,13} = N3$, and $N\beta_{1,14} = N4$. The other elements of the shape function are zero. The pertinent matrices for the mass, stiffness, and damping in terms of the shape functions are as follows.

For the mass matrix equation:

$$M_u = \bar{m} \int_0^l N_u^T N_u dr, \quad (32)$$

$$M_v = \bar{m} \int_0^l N_v^T N_v dr, \quad (33)$$

$$M_w = \bar{m} \int_0^l N_w^T N_w dr, \quad (34)$$

$$M_\beta = \bar{J}_m \int_0^l N_\beta^T N_\beta dr, \quad (35)$$

$$M_u = M_u + M_v + M_w + M_\beta. \quad (36)$$

For the stiffness matrix equations:

$$K_u = \bar{k}_x \int_0^l N_u^T N_u dr - (EA + \bar{m}B^2) \int_0^l \frac{\partial N_u^T}{\partial r} \frac{\partial N_u}{\partial r} dr - (\bar{m}a + B\bar{c}_x) \int_0^l N_u^T \frac{\partial N_u}{\partial r} dr, \quad (37)$$

$$K_v = \bar{k}_y \int_0^l N_v^T N_v dr + EI_z \int_0^l \frac{\partial^2 N_v^T}{\partial r^2} \frac{\partial^2 N_v}{\partial r^2} dr + \bar{m}B^2 \int_0^l N_v^T \frac{\partial^2 N_v}{\partial r^2} dr - (\bar{m}a + B\bar{c}_y) \int_0^l N_v^T \frac{\partial N_v}{\partial r} dr, \quad (38)$$

$$K_w = \bar{k}_z \int_0^l N_w^T N_w dr + EI_y \int_0^l \frac{\partial^2 N_w^T}{\partial r^2} \frac{\partial^2 N_w}{\partial r^2} dr + \bar{m}B^2 \int_0^l N_w^T \frac{\partial^2 N_w}{\partial r^2} dr - (\bar{m}a + B\bar{c}_z) \int_0^l N_w^T \frac{\partial N_w}{\partial r} dr - h\bar{k}_z \int_0^l N_w^T N_\beta dr, \quad (39)$$

$$K_\beta = (\bar{k}_t + \bar{k}_z h^2) \int_0^l N_\beta^T N_\beta dr + EI \int_0^l \frac{\partial^2 N_\beta^T}{\partial r^2} \frac{\partial^2 N_\beta}{\partial r^2} dr + (GJ + B^2 \bar{J}_m) \int_0^l N_\beta^T \frac{\partial^2 N_\beta}{\partial r^2} dr - (a\bar{J}_m + B\bar{c}_t) \int_0^l N_\beta^T \frac{\partial N_\beta}{\partial r} dr - 2\bar{k}_z h \int_0^l N_\beta^T N_w dr, \quad (40)$$

$$K_e = K_u + K_v + K_w + K_\beta. \quad (41)$$

Also, for the damping matrix equations:

$$C_u = \bar{c}_x \int_0^l N_u^T N_u dr - 2\bar{m}B \int_0^l N_u^T \frac{\partial N_u}{\partial r} dr, \quad (42)$$

$$C_v = \bar{c}_y \int_0^l N_v^T N_v dr - 2\bar{m}B \int_0^l N_v^T \frac{\partial N_v}{\partial r} dr, \quad (43)$$

$$C_w = \bar{c}_z \int_0^l N_w^T N_w dr - 2\bar{m}B \int_0^l N_w^T \frac{\partial N_w}{\partial r} dr, \quad (44)$$

$$C_\beta = \bar{c}_t \int_0^l N_\beta^T N_\beta dr - 2\bar{m}B \int_0^l N_\beta^T \frac{\partial N_\beta}{\partial r} dr, \quad (45)$$

$$C_e = C_u + C_v + C_w + C_\beta. \quad (46)$$

The inclusion of velocity V and acceleration a in the formulation causes the stiffness and damping matrices to be asymmetric.

According to equations (39) and (40), it is obvious that the rail interacts with the lateral and the torsional deflections. This is because of the traverses' locations which are under the rail and do not contact the shear forces. The traverses have a distance equal to h from the shear center of the rail. This eccentricity affects the stiffness matrix, not the mass and damping matrices. It can be shown by

$(-h\bar{k}_z \int_0^l N_w^T N_\beta dr)$ parameter in the K_w formulation and by $((\bar{k}_t + \bar{k}_z h^2) \int_0^l N_\beta^T N_\beta dr - 2\bar{k}_z h \int_0^l N_\beta^T N_w dr)$ parameter in the K_β formulation. This is so important in the earthquake calculation which determines the effect of the lateral and torsional deflection modes on rail response.

3. Numerical Results

Using the formulation described here, the numerical solution was carried out in a mathematical program for the case of constant acceleration using the Newmark β method taking $\Delta t = 0.001$ s. Since similar studies have been done just in vertical direction by Koh et al. [7] and Tran et al. [8] using moving elements, the first numerical examples were compared with their results to verify the developed formulations. They used common finite elements; therefore, comparison can establish the validity and effectiveness of the macroelement used in the present study.

Figure 4(a) shows the deflected shape of the track as a beam model obtained by Koh [7] and that for the current study using the same track properties. The results were in good agreement.

According to Figure 4(b), displacement tends to zero in a very short distance away from the point of application of the force. However, in a small length of the rail, this value is

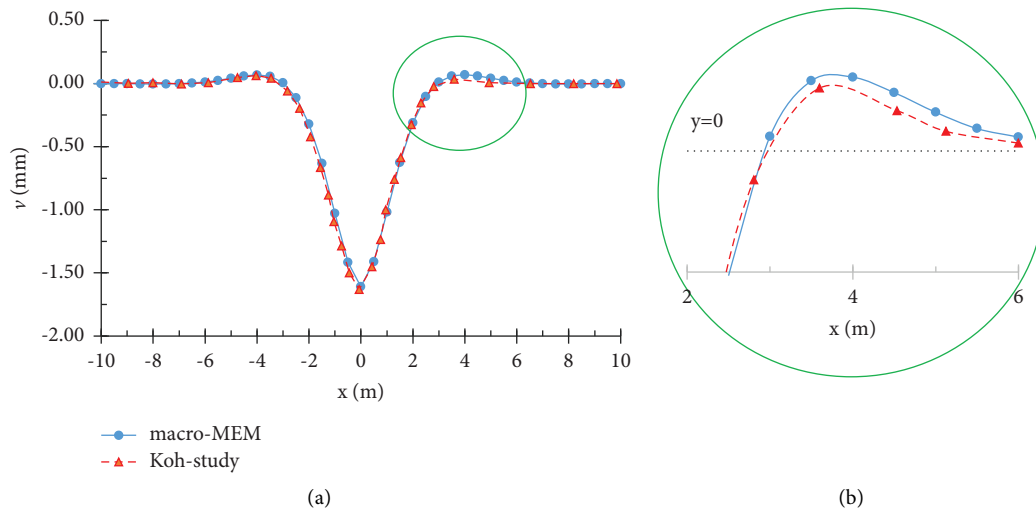


FIGURE 4: Verification of rail deflection under concentrated load with Koh's study [7].

set positive which can be attributed to occurrence of a weak uplift in the rail structure.

In Figure 5, the effect of two wagons with moving loads (2 concentrated loads at each wagon) on the railroad is evaluated. Interaction effect of the loads can readily be compared to the model with a single concentrated load.

Determining the correct dimension of the model is important for infinite domains so that the boundary effects do not invalidate the results. These dimensions are usually established by trial and error. The use of moving elements ensures that the load (moving train) will never approach the boundaries. However, the response of the loads applied at points on the track that are distant from the boundary must be negligible at the latter point. To ensure this, the length of the track must be determined in a way that the displacement response, velocity, and acceleration response will be negligible at the boundary. In order to avoid the shock of an abrupt load, the constant axial load is applied gradually from zero to its maximum value over a time span of one second, after which the load remains constant.

In Figure 6, the effect of boundary conditions on acceleration response of the railroad can obviously be seen. Although boundary conditions do not affect displacement response of the railroad when using the moving coordinate method, their impact on acceleration response cannot be neglected.

Figure 7 shows the velocity and acceleration of the track vibration at the end of the load period. These graphs were prepared for a constant track velocity of 80 km/h. For different ranges of train speed, the maximum velocity and acceleration of the track vibration occur in a 0.07 to 0.35 length of track at the midpoint and in a time span of 0.4 to 0.6 of the total loading time. The distance of the points, where the maximum velocity and acceleration occur, increases in front of the location of the load with the increasing speed of the train (as the train speed increases, the point experiencing maximum vibration velocity and acceleration is at a distance from the load point). This happens because of the decrease in interference by waves at high train speeds.

Train speed is a major parameter affecting the response of the track and is important in track design and maintenance. On Iranian lines, this speed is usually 80 km/h for freight trains and 100 to 160 km/h for passenger trains. For high-speed trains, the speed is usually over 200 km/h. In the current study, the speed varied from 80 to 300 km/h to demonstrate the full range of this parameter. For fast moving trains, the tracks have higher strength, which must be reflected in the track properties.

Figure 8 shows the effect of train speed on the response of the track. This graph shows the maximum response at the midpoint of the track under the point load. The maximum vibration velocity and acceleration at the midpoint occur at $t = 0.06$ to 1.0 s during load passing at different velocities. Figure 8(a) shows that an increase in train speed which had little effect on the maximum deflection of the track, but caused decreases in the track vibration velocity and acceleration, occurred in response to the effect of the moving load. The effect of train velocity on the track vibration response is shown in Figures 8(b) and 8(c).

Because the response of the track is affected by the speed of the train, it is necessary to choose an appropriate length for the model. Figure 9 shows the response at the boundary of the model for different train speeds. It is evident that dampening the effect of acceleration at the boundary is more difficult. Figure 9(a) shows that the track deflection for each length analyzed will fall to zero at the boundary points; however, the vibration velocity and acceleration of the track do not (Figures 9(b) and 9(c)). Since at the points where the displacement is equal to zero and assumed as the end point, the rail still has vibrational acceleration, the length of the computational model should be determined by the acceleration status of the end point of the model and not by the displacement of this point. The best track length for dampening of the vibration acceleration at the boundary points is over 350 m, where both the acceleration and velocity fall to zero. To model the boundary conditions of the rail, it is more effective to use springs at the boundary points that have

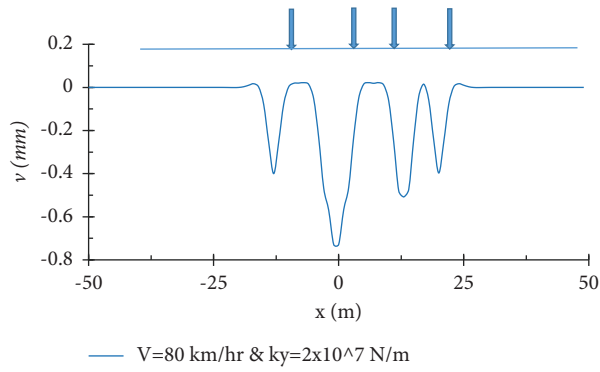


FIGURE 5: Rail deflection response under two wagons simulated by point loads.

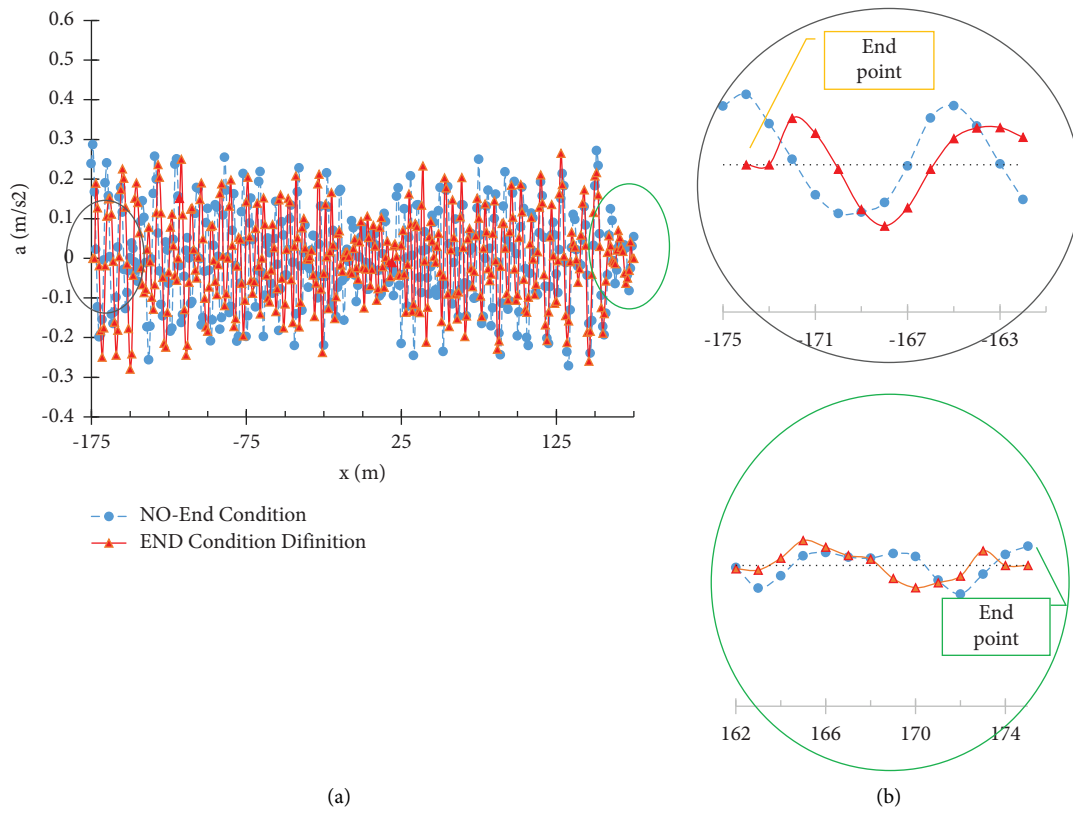


FIGURE 6: Comparison of acceleration response with definition of boundary conditions.

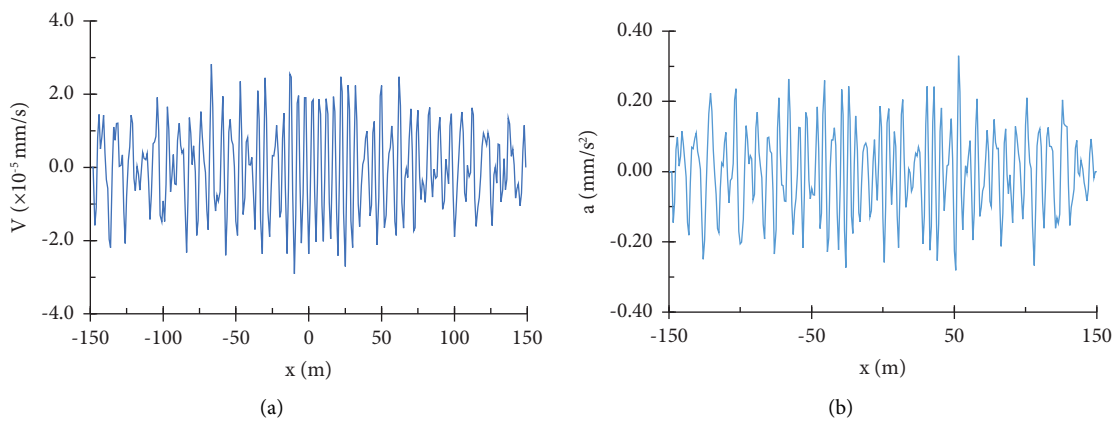


FIGURE 7: Track velocity and acceleration vibrational response for train velocity = 80 km/hr. (a) Velocity. (b) Acceleration.

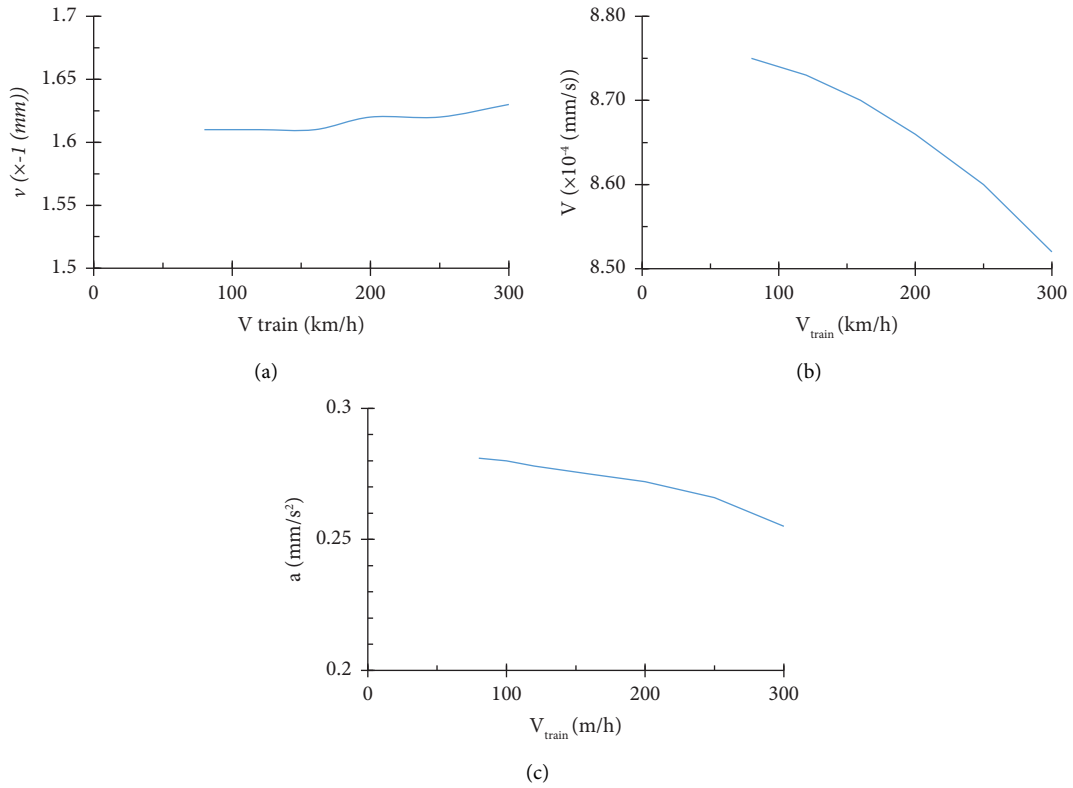


FIGURE 8: Response at midpoint of the track for different train speeds: (a) track max vertical deflection; (b) track max vertical velocity; (c) track vertical acceleration.

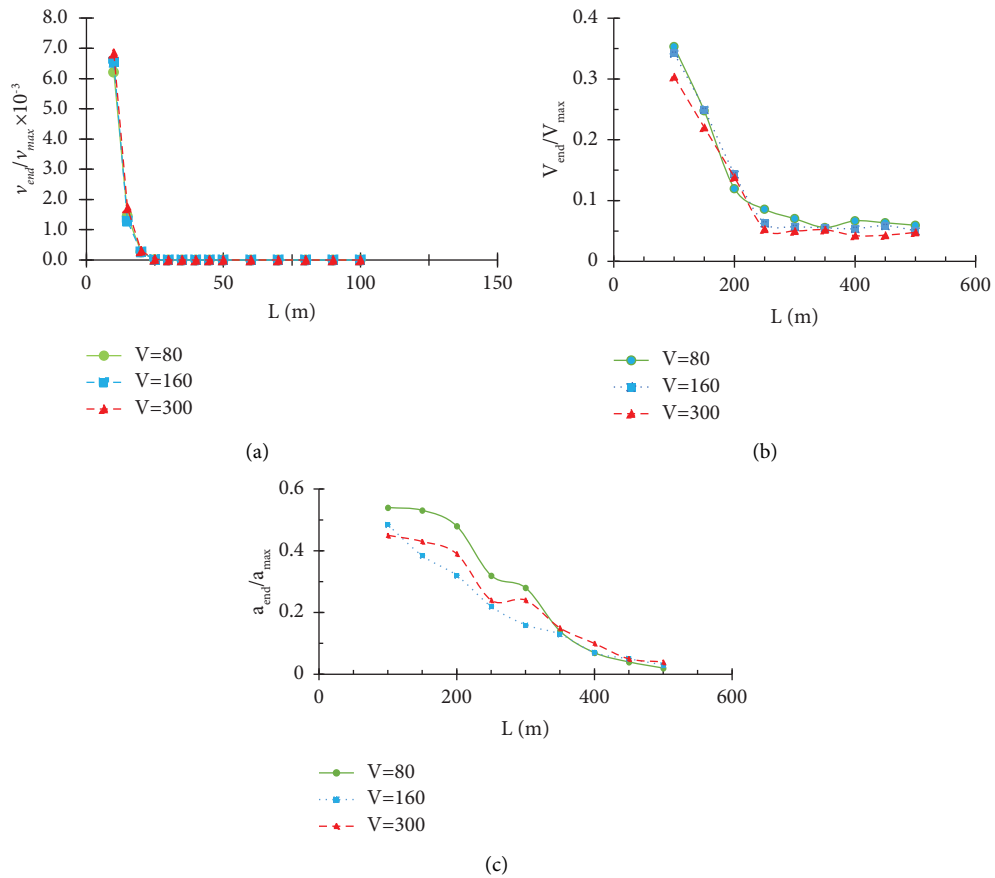


FIGURE 9: Ratio of end response to maximum response of the beam model. (a) Deflection. (b) Velocity. (c) Acceleration.

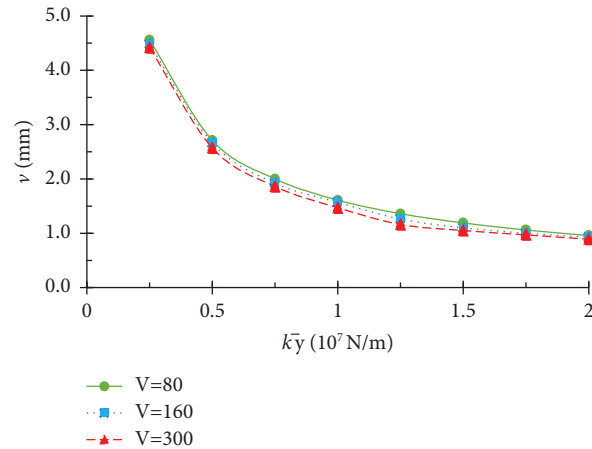


FIGURE 10: Midpoint deflection of rail vs. bed stiffness.

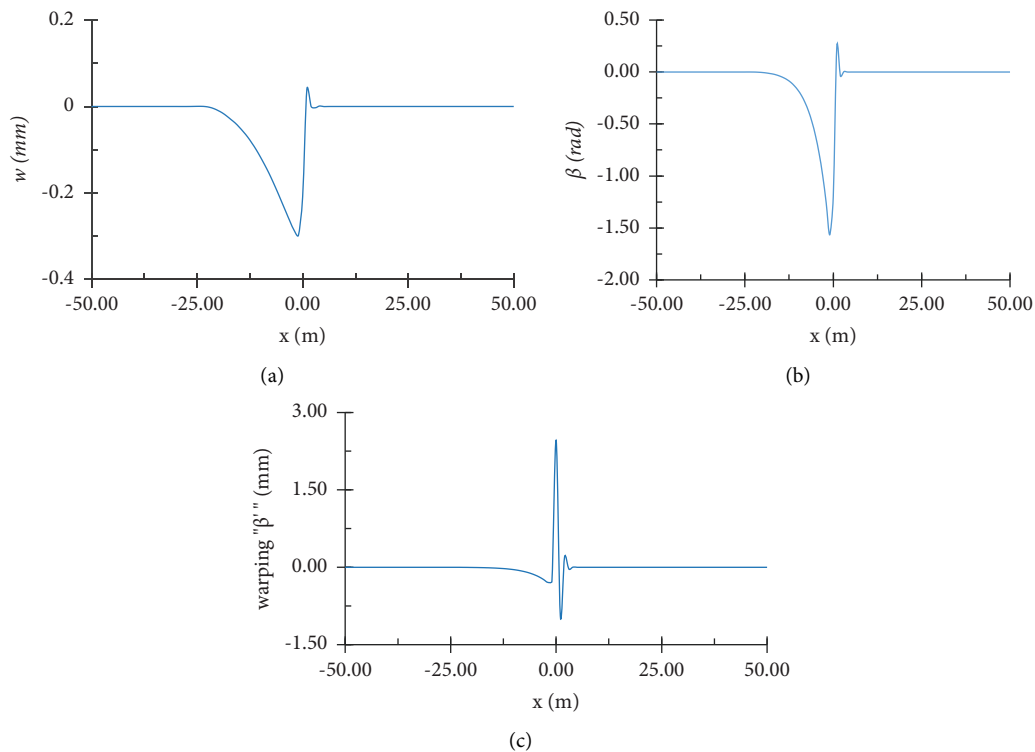


FIGURE 11: Track lateral deflection rotation angle and warping value response for moving lateral concentrated load velocity = 80 km/hr. (a) Track lateral deflection. (b) Track rotation angle. (c) Track warping value.

a stiffness equivalent to that of semi-infinite beam. The boundary response under such conditions is more accurate than for other forms, such as for fixing the boundary points or lack of definition of the boundaries.

Figure 10 shows the effect of the rail bed stiffness on deflection of the rail at different velocities. The bed stiffness varied from $\bar{k} = 0.25 \times 10^7 \text{ N/m}$ for a soft bed to $\bar{k} = 2.0 \times 10^7 \text{ N/m}$ for the hardest bed. The rate of variation of deflection of the railroad under the point load at $\bar{k} \geq 1.25 \times 10^7 \text{ N/m}$ decreased more slowly than that under soft bed conditions. It was also independent of load velocity, as

shown in Figure 8(a). As stated, a change in train velocity had no effect on the deflection response of the track. The deflection of the track depended on the bed stiffness as the external condition and rail properties as the internal parameters of the model.

The interaction of lateral degree of freedom along Z and the torsion and warping created in the model due to the eccentricity of stiffness and shear centers are of the most important modes in studying the vibration diagrams of a beam on elastic foundation which is also mentioned in the formulation. In order to investigate the governing

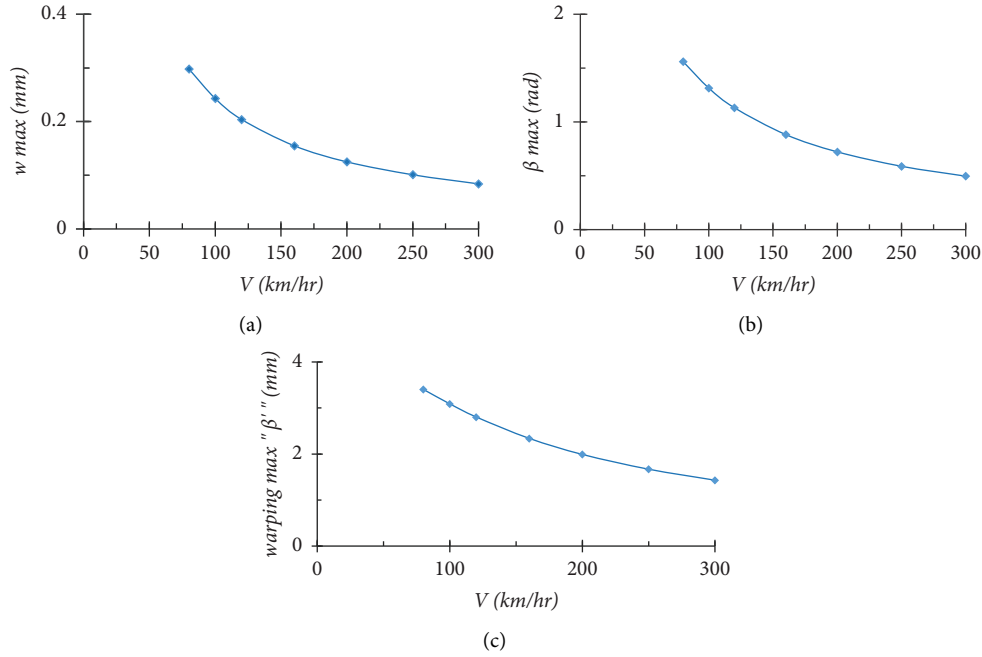


FIGURE 12: Track maximum response in the separate DoFs in the midpoint under moving lateral concentrated load with different velocities. (a) Maximum lateral deflection. (b) Maximum rotational angle. (c) Maximum warping value.

interaction conditions of the modeled beam, a concentrated force $F = 6 \times 10^3 \text{ Kg}$ is applied to the midpoint of the rail. Figures 11 and 12 examine the interactional response of the rail in the degrees of freedom related to lateral displacement, torsion, and warping due to the presence of coupled stiffness matrices. According to equations (39) and (40), by applying force in the lateral degree of freedom, w , the values of torsion and warping along the rail can be attained. The length of the rail beam is modeled to be above 200 meters to investigate the interaction of lateral and torsional degrees of freedom. Also, the speed of the lateral concentrated load on the rail is assumed to be similar to the speeds required for the vertical mode. In the results, only the diagram for a part of the rail with a significant vibration amplitude is shown. The diagrams of Figure 11 show the changes in lateral displacement, torsion angle, and warping of the rail beam model. In these diagrams, the concentrated lateral load's speed is assumed to be 80 km/hr. According to the diagrams, the maximum lateral displacement of 0.3 mm, the maximum torsion angle of 1.57 radians, and the maximum warping on the rail equal to 2.46 mm were observed for the speed of 80 km/hr. Also, the changes in the values of lateral displacement, torsion, and warping of the rail beam model for different load speeds are presented in Figure 12. Besides, the reduction of the parameters with the increased concentrated moving load's speed can be seen clearly. In the calculations related to the involved degrees of freedom in question, the changes of stiffness in different modes are not considered.

Regarding the dynamic impact of a train on the railroad, it can be simulated as a sinusoidal harmonic load with different dynamic frequencies. Thus, the frequency of the load can be considered as a variable in the analysis. The general form of the equation is (see Figure 13)

$$P(t) = P_0 \sin(\omega t). \quad (47)$$

Dynamic amplification factor (DAF) is considered as a fundamental parameter in vibration analysis of the railroads. Herein, DAF is defined as the ratio of the maximum dynamic deformation to maximum static deformation in the point of application of the concentrated force.

According to Figure 14, dynamic amplification factor is maximal for the load with vibration frequency of $\omega = 2.5$. Consequently, it can lead to resonance in the vibration of the rail. Besides, increasing the load frequency results in a decrease in DAF. Here, calculation was performed at the point of application of the force.

In order to investigate the effect of bed stiffness on DAF, AR index is defined as follows:

$$AR = \left| \frac{DAF_{\bar{k}_y} - DAF_{\bar{k}_y=1 \times 10^7}}{DAF_{\bar{k}_y=1 \times 10^7}} \times 100 \right|, \quad (48)$$

where DAF_{k_y} is the equivalent dynamic amplification factor of k_y and $DAF_{k_y=1 \times 10^7}$ is the equivalent dynamic amplification of $K_y = 1 \times 10^7 \text{ N/m}$, which was used as the base value of the bed stiffness in the previous studies [7].

Figure 15 shows AR variation vs. bed stiffness for three different harmonic load frequencies. As it can be observed, the ratio is maximal when $\bar{k}_y = 0.35 \times 10^7 \text{ N/m}$ and it can be interpreted as occurring resonance in the vibrational response of the rail.

Since the acceleration of the motion of load has no significant effect on the vibrational results of the model [8], in the numerical results of this study, the results of concentrated load acceleration are considered equal to zero. Also, due to the general similarity of the formulations in

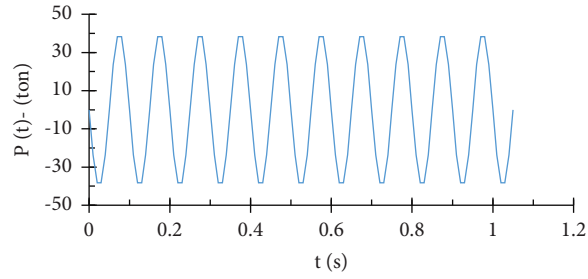


FIGURE 13: Harmonic load graph.

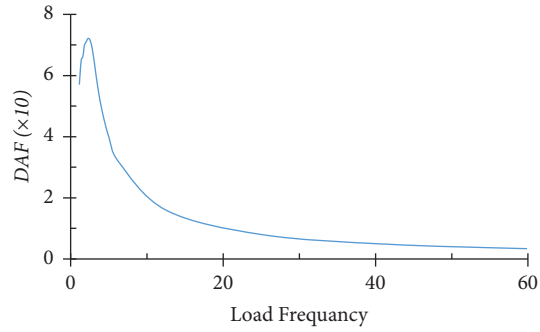


FIGURE 14: Railroad dynamic amplification factor due to different frequencies of the harmonic load.

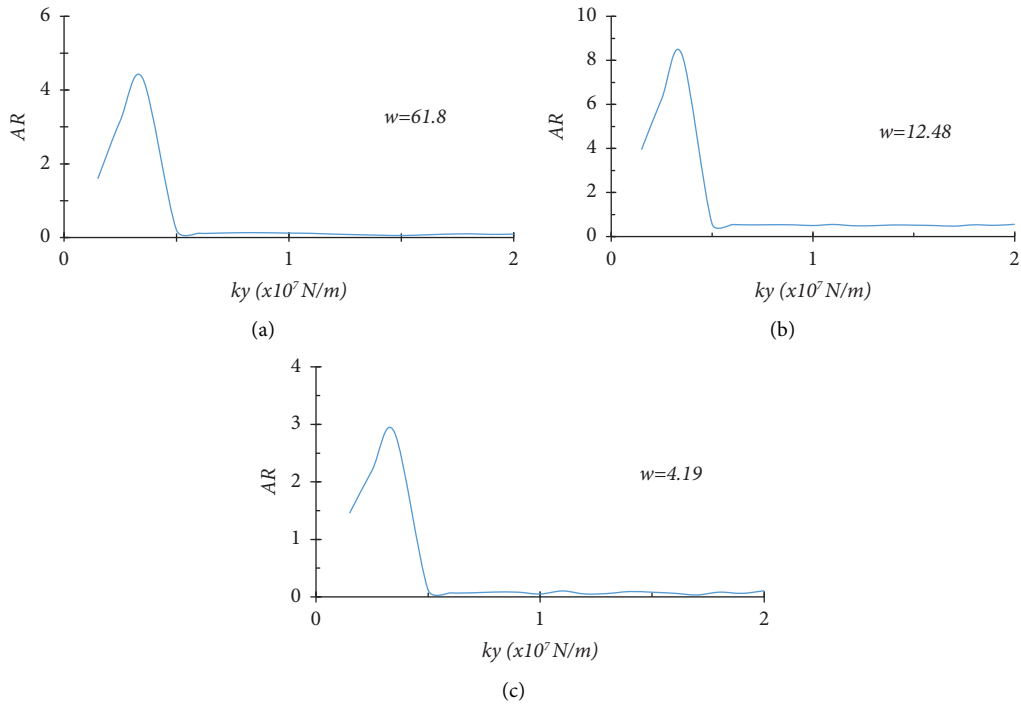


FIGURE 15: Variation rate of the DAF (AR parameter) vs. bed stiffness.

different DoFs, only the effective parameters in the numerical results related to the two vertical directions and the effect of the lateral point load on the lateral response of the system and the torsion angle as well as warping DoF were evaluated.

4. Motivation and Contribution

The most important motivation in this research is to create a comprehensive model to analyze the beam on the elastic bed under the effect of moving loads. One of the basic factors in modeling is examining the interaction of degrees of freedom for simultaneous analysis of loads. The most important advantage of the current model is the significant reduction in calculation time, which allows to use the characteristic matrices obtained in the results by commercial software.

5. Managerial Insight

The macroelement introduced in this article does not have the ability to be used in the arch, and thus the relevant formulation should be modified in this context. Also, if there is a departure from the center of the load with respect to the y axis, its effect should be considered manually. Another shortcoming of the current model is the lack of investigation of nonlinear effects in the soil under the model and in the rail track itself, which are recommended to be investigated in future research and to develop the current model. For the next research, the effects of rail corrugation and the geometric nonlinearity effects of the model as well as the effects of soil interaction and soil paste conditions are suggested to be investigated. Therefore, the project managers in railroad construction can take advantage of our findings to make their plans more viable.

6. Conclusion

We aimed to introduce and develop a macroelement model for analyzing structures under the influence of moving load and relying on railroad structure. For this purpose, with the help of the moving element, the response of the rail structure was studied. The formulation was regulated based on the minimum potential energy and Galerkin method, and stiffness, mass, and damping matrices for moving macroelements were formed accordingly. Some of the matrices became asymmetric due to the speed of the concentrated load (train). The Newmark β numerical method was adopted to analyze the results in medium acceleration mode. The parameters studied in this regard are length of the model, effect of train speed, and also the rail response to lateral point load to evaluate the capability of the model.

In this study, in order to evaluate the effect of passenger and freight trains according to the conditions of Iranian trains, different train speeds are considered. The important achievement of this research is the direct relationship between the length and boundary conditions of the computational model and the vibrational acceleration of the beam model.

The vibrational responses of rails including displacement, velocity, and vibrational acceleration depend on the environmental conditions of the model, such as bed conditions, material properties, and rail cross-sectional characteristics. The interaction of the lateral transitional and torsional degree of freedom and consequent warping is amongst the other findings of this study, which is very important in seismic evaluation of rails.

Data Availability

The data used to support the findings of this study are available from the corresponding author upon request.

Conflicts of Interest

The authors declare that they have no conflicts of interest.

References

- [1] C. Steele, "The finite beam with a moving load," *Journal of Applied Mechanics*, vol. 34, no. 1, pp. 111–118, 1967.
- [2] E. Touti and A. P. Chobar, "Utilization of AHP and MCDM integrated methods in urban project management (A case study for eslamshahr-tehran)," *International journal of industrial engineering and operational research*, vol. 2, no. 1, pp. 16–27, 2020.
- [3] L. Fryba, *Vibration of Solids and Structures under Moving Loads*, Springer Science and Business Media, Berlin, Germany, 3 edition, 1999.
- [4] L. Fryba, S. Nakagiri, and N. Yoshikawa, "Stochastic finite elements for a beam on a random foundation with uncertain damping under a moving force," *Journal of Sound and Vibration*, vol. 163, no. 1, pp. 31–45, 1993.
- [5] Y. H. Chen and Y. H. Huang, "Dynamic stiffness of infinite Timoshenko beam on viscoelastic foundation in moving coordinate," *International Journal for Numerical Methods in Engineering*, vol. 48, no. 1, pp. 1–18, 2000.
- [6] L. Andersen, S. R. Nielsen, and P. Kirkegaard, "Finite element modelling of infinite Euler beams on Kelvin foundations exposed to moving load in convected co-ordinates," *Journal of Sound and Vibration*, vol. 241, no. 4, pp. 587–604, 2001.
- [7] C. Koh, J. S. Y. Ong, D. K. H. Chua, and J. Feng, "Moving element method for train-track dynamics," *International Journal for Numerical Methods in Engineering*, vol. 56, no. 11, pp. 1549–1567, 2003.
- [8] M. T. Tran, K. K. Ang, and V. H. Luong, "Vertical dynamic response of non-uniform motion of high-speed rails," *Journal of Sound and Vibration*, vol. 333, no. 21, pp. 5427–5442, 2014.
- [9] P. M. Mathews, "Vibration of a beam on elastic foundation," *ZAMM - Zeitschrift für Angewandte Mathematik und Mechanik*, vol. 38, no. 3-4, pp. 105–115, 1958.
- [10] L. Jezequel, "Response of periodic systems to a moving load," *Journal of Applied Mechanics*, vol. 48, no. 3, pp. 613–618, 1981.
- [11] K. Ono and M. Yamada, "Analysis of railway track vibration," *Journal of Sound and Vibration*, vol. 130, no. 2, pp. 269–297, 1989.
- [12] A. Trochanis, R. Chelliah, and J. Bielak, "Unified approach for beams on elastic foundations under moving loads," *Journal of Geotechnical engineering*, vol. 113, no. 8, pp. 879–895, 1987.

- [13] F. F. Calm, "Forced vibration of curved beams on two-parameter elastic foundation," *Applied Mathematical Modelling*, vol. 36, no. 3, pp. 964–973, 2012.
- [14] J. Dai, M. Han, and K. K. Ang, "Moving element analysis of partially filled freight trains subject to abrupt braking," *International Journal of Mechanical Sciences*, vol. 151, pp. 85–94, 2019.
- [15] V. Nguyen and D. Duhamel, "Finite element procedures for nonlinear structures in moving coordinates. Part 1: infinite bar under moving axial loads," *Computers and Structures*, vol. 84, no. 21, pp. 1368–1380, 2006.
- [16] V. Nguyen and D. Duhamel, "Finite element procedures for nonlinear structures in moving coordinates. Part II: infinite beam under moving harmonic loads," *Computers and Structures*, vol. 86, no. 21–22, pp. 2056–2063, 2008.
- [17] T. P. Nguyen, D. T. Pham, and P. Hoang, "A new foundation model for dynamic analysis of beams on nonlinear foundation subjected to a moving mass," *Procedia Engineering*, vol. 142, pp. 166–173, 2016.
- [18] G. Kouroussis and O. Verlinden, "Prediction of railway ground vibrations: a," *Soil Dynamics and Earthquake Engineering*, vol. 69, pp. 220–226, 2015.
- [19] P. A. Ferreira and A. López-Pita, "Numerical modelling of high-speed train/track system for the reduction of vibration levels and maintenance needs of railway tracks," *Contents lists available at ScienceDirect Construction and Building Materials*, vol. 79, pp. 14–21, 2015.
- [20] J. A. Zakeri and H. Xia, "Sensitivity analysis of track parameters on train-track dynamic interaction," *Journal of Mechanical Science and Technology*, vol. 22, no. 7, pp. 1299–1304, 2008.
- [21] V. Sarvestan, H. R. Mirdamadi, and M. Ghayour, "Vibration analysis of cracked Timoshenko beam under moving load with constant velocity and acceleration by spectral finite element method," *International Journal of Mechanical Sciences*, vol. 122, pp. 318–330, 2017.
- [22] R. U. A. Uzzal, R. B. Bhat, W. Ahmed, and W. Ahmed, "Dynamic response of a beam subjected to moving load and moving mass supported by Pasternak foundation," *Shock and Vibration*, vol. 19, no. 2, pp. 205–220, 2012.
- [23] H. Hua, M. Qiu, and Z. Liao, "Dynamic analysis of an axially moving beam subject to inner pressure using finite element method," *Journal of Mechanical Science and Technology*, vol. 31, no. 6, pp. 2663–2670, 2017.
- [24] G. Mei, C. Yang, S. Liang et al., "A reduced time-varying model for a long beam on elastic foundation under moving loads," *Journal of Mechanical Science and Technology*, vol. 32, no. 9, pp. 4017–4024, 2018.
- [25] A. Jahangiri, N. K. A. Attari, A. Nikkhoo, and Z. Waezi, "Nonlinear dynamic response of an Euler–Bernoulli beam under a moving mass–spring with large oscillations," *Archive of Applied Mechanics*, vol. 90, no. 5, pp. 1135–1156, 2020.
- [26] H. D. Phadke and O. R. Jaiswal, "Dynamic response of railway track resting on variable foundation using finite element method," *Arabian Journal for Science and Engineering*, vol. 45, no. 6, pp. 4823–4841, 2020.
- [27] D. Froio, E. Rizzi, F. M. Simões, and A. Pinto da Costa, "Critical velocities of a beam on nonlinear elastic foundation under harmonic moving load," *Procedia Engineering*, vol. 199, pp. 2585–2590, 2017.
- [28] E. Looi and F. Arbabi, "Stability and dynamic response of railroad tracks under stochastic loads," vol. 2, M.S. Thesis, 1987.
- [29] F. Arbabi, A. Sherbourne, and H. El-Ghazaly, "Strength and deflection of railway tracks -I: probabilistic finite element analysis," *Computers and Structures*, vol. 39, no. 1–2, pp. 9–21, 1991.
- [30] F. Li and F. Arbabi, "Stability and dynamic response of railroad tracks under stochastic loads," vol. 1, M.S. thesis, 1987.
- [31] F. Arbabi and C. U. Loh, "Reliability analysis of railroad tracks," *Journal of Structural Engineering*, vol. 117, no. 5, pp. 1435–1447, 1991.
- [32] M. Abolghasemian, A. P. Chobar, M. AliBakhshi, A. Fakhr, and S. Moradi, "Delay scheduling based on discrete-event simulation for construction projects," *Iranian Journal of Operations Research*, vol. 12, no. 1, pp. 49–63, 2021.
- [33] F. Arbabi, "Variational formulation of rail overturning, Part 4, structural dynamics, systems identification. Computer amplifications. Shock and vibration," *Bulletin*, vol. 47, pp. 149–154, 1977.
- [34] *National Iranian Trade Journal Number 301*, Public Technical Characteristics of Superstructure of railroad, Tehran, Iran, 2005.
- [35] W. McGuire, R. Gallagher, and R. Ziemian, *Matrix Structural Analysis*, John Wiley and Sons. Inc, New York, NY, USA, 2000.
- [36] A. V. Metrikine and H. A. Dieterman, "Instability of vibrations of a mass moving uniformly along an axially compressed beam on a viscoelastic foundation," *Journal of Sound and Vibration*, vol. 201, no. 5, pp. 567–576, 1997.
- [37] S. Timoshenko, *Strength of Materials Part II: Advanced Theory and Problems*, Nine printing, van Nostrand, New York, NY, USA, 2 edition, 1940.